AD-A081 578 NORTH TEXAS STATE UNIV DENTON DEPT OF PHYSICS F/G 20/12
INVESTIGATION OF LASER OPTICAL BIASING ON THE QUANTUM TRANSPORT--ETC(U)
OCT 79 D G SEILER N00014-76-C-0319

UNCLASSIFIED NL

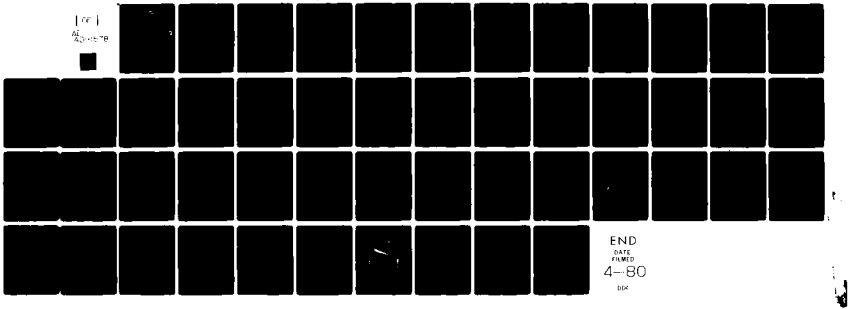

END
DATE FILMED
4-80
DDC

12

ANNUAL SUMMARY REPORT

Investigation of Laser Optical Biasing on the Quantum Transport Properties of n-InSb

by

David G. Seiler

Department of Physics

North Texas State University

Denton, Texas 76203

October 1, 1978 - September 30, 1979

Prepared for the Office of Naval Research
Electronic and Solid State Sciences Program
Under Contract NR 318-039

SECURITY CLASSIFICATION OF THIS PAGE *(When Data Entered)*

REPORT DOCUMENTATION PAGE		READ INSTRUCTIONS BEFORE COMPLETING FORM
1. REPORT NUMBER	2. GOVT ACCESSION NO.	3. RECIPIENT'S CATALOG NUMBER
4. TITLE *(and Subtitle)* LASER OPTICAL BIASING OF THE QUANTUM TRANSPORT PROPERTIES OF n-InSb AD631161		5. TYPE OF REPORT & PERIOD COVERED 1 Oct. 1978 - 30 Sept. 1979 6. PERFORMING ORG. REPORT NUMBER
7. AUTHOR(s) DAVID G. SEILER		8. CONTRACT OR GRANT NUMBER(s) N00014-76-C-0319 ✓
9. PERFORMING ORGANIZATION NAME AND ADDRESS DEPARTMENT OF PHYSICS ✓ NORTH TEXAS STATE UNIVERSITY DENTON, TEXAS 76203		10. PROGRAM ELEMENT, PROJECT, TASK AREA & WORK UNIT NUMBERS
11. CONTROLLING OFFICE NAME AND ADDRESS ONR Electronic and Solid State Sciences Program Office of Naval Research Arlington, VA 22217		12. REPORT DATE October, 1979 13. NUMBER OF PAGES 48 pages
14. MONITORING AGENCY NAME & ADDRESS *(if different from Controlling Office)* ONR Resident Representative 528 Federal Building 300 East 8th Street Austin, Texas 78701		15. SECURITY CLASS. *(of this report)* Unclassified 15a. DECLASSIFICATION/DOWNGRADING SCHEDULE

16. DISTRIBUTION STATEMENT *(of this Report)*

This document has been approved for public release and sale; its distribution is unlimited.

17. DISTRIBUTION STATEMENT *(of the abstract entered in Block 20, if different from Report)*

18. SUPPLEMENTARY NOTES

19. KEY WORDS *(Continue on reverse side if necessary and identify by block number)*

InSb	Magneto-optical properties
Quantum Transport	Interaction of laser radiation with semiconductors
Optical Biasing	CO_2 Laser
Photoexcited carriers	CO Laser
Photoconductivity	

20. ABSTRACT *(Continue on reverse side if necessary and identify by block number)*

The interaction of CO_2 and CO laser radiation with the semiconductor InSb has been studied at liquid helium temperatures with a highly sensitive photoconductive technique. Two distinct sets of resonant magnetophotoconductivity structure have been observed and identified as arising from multiphonon assisted cyclotron harmonic transitions and impurity level transitions. The first observation of a laser induced cooling process of the conduction electrons in n-InSb has been made using a CO laser and an applied dc electric field.

DD FORM 1 JAN 73 1473 EDITION OF 1 NOV 65 IS OBSOLETE

SUMMARY

In this annual summary report a description of the theoretical and experimental progress in the investigation of laser optical biasing effects on the quantum transport properties of n-InSb is given for the period October 1, 1978 - September 30, 1979.

Reprints and preprints of papers worked on and published during this time span are reproduced in this report.

These papers are:

PHOTOCONDUCTIVITY OF LASER EXCITED HOT ELECTRONS IN DEGENERATE n-InSb*

D G Seiler, J R Barker, B T Moore, and K E Hansen
Department of Physics, North Texas State University
Denton, Texas 76203

CO_2 laser-induced hot carrier and free carrier absorption effects are investigated at 1.8 K. Electron temperatures are extracted for various laser frequencies and powers. Parallel photo- and electrical heating experiments provide information about the photoexcitation and hot carrier generation process.

Optical heating of carriers in semiconductors illuminated by intense laser radiation has been extensively studied with transmission or photoluminescence measurements. Here we examine CO_2 laser-induced heating of electrons in degenerate n-InSb at liquid helium temperatures by investigating the corresponding conductivity changes. The free carrier absorption of this CO_2 laser radiation is thus shown to be a valuable new tool for the extraction of information on photo-heated hot carriers.

The sample of n-InSb, immersed in liquid helium at 1.8 K, was illuminated with a laser pulse produced by mechanically chopping a beam (TEM_{00} mode) from a grating-tuned cw CO_2 laser. The laser pulse had a width of ~20 μsec (F.W.H.M.), a rise and fall time of ~2 μsec, repetition rate of 1700 Hz, and a peak power of several watts over a number of lines between 9.2 and 10.8 μm. Calibrated filters of either CaF_2 or BaF_2 were used after the chopper for beam attenuation.

Figures 1(a), (b) and (c) show results of three separate experiments on how the mobility ratio μ/μ_0 changes with (a) applied electrical power per electron $P_E(=e\mu E^2)$; (b) lattice temperature T_L; (c) peak incident laser power P_I. The electron concentration (1.4×10^{15} cm^{-3}) is constant at these lattice temperatures and low laser powers where two-photon absorption processes are completely negligible. Consequently, the measured changes in conductivity are simply related to the changes in mobility. As seen in Fig. 1(b), the mobility increases with lattice temperature, T_L, which is consistent with dominant ionized impurity momentum relaxation. Pulsed dc electric fields of 20 μsec duration were used to electrically heat the carriers into the warm electron region as shown in Fig. 1(a) for zero laser power. Additional mobility ratio data were taken at higher values of T_L and P_E

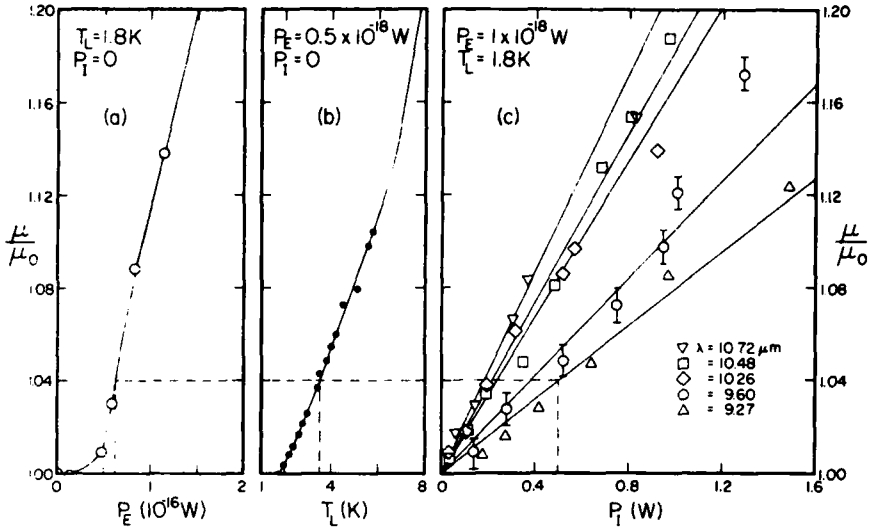

Fig. 1. Mobility changes with (a) P_E, (b) T_L, and (c) P_I.

than are shown on these two plots. The CO_2 laser radiation is partially absorbed via free carrier absorption processes which subsequently leads to a mobility increase as seen in Fig. 1(c) where μ/μ_0 is plotted versus P_I. The laser beam was positioned to illuminate the region of the sample between the potential contacts. In all cases the beam diameter was larger than the width of the sample, but smaller than the distance between the potential leads. From the measured voltage drop across the leads, which contain resistances from both illuminated and unilluminated regions and geometrical considerations of the laser spot size, one can calculate the mobility of only the illuminated region. It is this mobility μ which is plotted in Fig. 1(c).

Electron temperatures can be determined for each wavelength and value of P_I by making a one-to-one correspondence between the mobility changes in the two cases shown in Fig. 1(b) and (c). For example, for λ=9.27 μm and P_I=0.5 W, μ/μ_0=1.04 which corresponds to the same mobility ratio for a temperature T_L=3.5 K. Provided the steady state is controlled by intercarrier collisions, the carrier distribution will be a heated Fermi-Dirac distribution with a true electron temperature T_e if the carrier heating maintains the system within the regime dominated by ionized impurity limited mobilities. A plot of T_e versus P_I

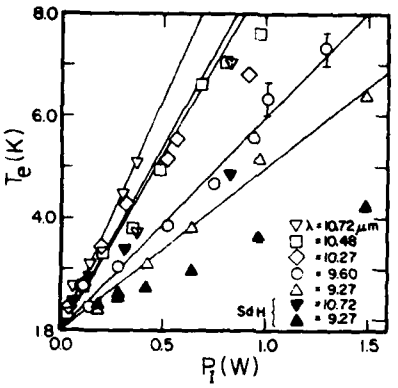

Fig. 2. T_e versus P_I for several CO_2 laser wavelengths.

is shown in Fig. 2.

We have estimated the initial carrier concentration n_c^* for which the energy loss rate $\Gamma_{ee}(\varepsilon)$ (scattering out) due to an excited electron of high energy ε scattering against the background carriers equals the energy loss rate $\Gamma_{eph}(\varepsilon)$ due to phonon scattering using a similar calculation to Stratton but allowing for the degeneracy of the low energy carrier distribution and Thomas-Fermi screening. For the present sample, $n<<n_c^*\sim10^{18}$ cm^{-3}, for energies $\varepsilon>>\varepsilon_F+\hbar\omega_L$, where energy loss is controlled by polar mode optic phonon emission (phonon energy, $\hbar\omega_L$). However, for $\varepsilon<\varepsilon_F+\hbar\omega_L$, $n>>n_c\sim10^{14}$ cm^{-3}, where n_c is the electron concentration for a valid electron temperature model computed using a modified Hearn criterion.

We assume therefore that a fraction β of the optically absorbed power $P_a^o=\alpha dP_I$ (Multiple reflections, but not interference effects, are taken into account here. The sample thickness is d, α is the free carrier absorption coefficient and $\alpha d<<1$.) is transferred to the lattice by optic phonon cascading as the photoexcited electrons scatter to energies below the threshold, $\varepsilon\sim\varepsilon_F+\hbar\omega_L$ for which $\Gamma_{eph}>\Gamma_{ee}$. The residual power $P_a=[1-\beta(\lambda)]P_a^o$ is then effective in heating the carriers into a Fermi-Dirac distribution with electron temperature T_e via intercarrier collisions. The subsequent quasi-thermalized distribution will then lose energy to the lattice via predominantly acoustic phonon processes at the rate $[1-\beta(\lambda)]P_a^o$.

By comparing the power balance in the electric field and separate laser heating experiments, we are able to extract an effective free carrier absorption coefficient α_{eff}, related to the true value $\alpha(\lambda,T_e)$ by $\alpha_{eff}=[(1-\beta(\lambda)]\alpha(\lambda,T_e)$ and determined experimentally by the ratio $\alpha_{eff}=P_E(T_e)/dP_i(T_e,\lambda)$. $P_E(T_e)$, as defined previously, is the electrical power per electron producing an electron temperature T_e at zero laser power and $P_i(T_e,\lambda)$ is the incident laser power per

illuminated electron. For samples with $n>n_c^*$, we have $\beta=0$ where $\alpha_{eff}=\alpha$ and a precision extraction of the true absorption coefficient becomes possible.

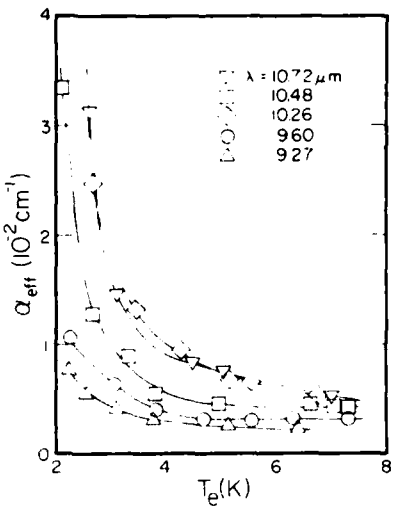

Fig. 3. α_{eff} versus T_e for several values of λ.

Figure 3 shows the variation of α_{eff} with T_e for different constant values of λ for which we expect β=constant. The behavior of α_{eff} can be understood from energy balance considerations for a degenerate electron gas where $\alpha_{eff}=\Delta\varepsilon(T_e)/dP_i\tau_\varepsilon$ and τ_ε is the phenomenological energy relaxation time and $\Delta\varepsilon(T_e)=\varepsilon(T_e)-\varepsilon(T_L)$ where $\varepsilon(T)$ is the average energy of an electron. The variation of this phenomenological energy relaxation time with electron temperature is the cause of this strong electron temperature dependence of α_{eff}.

A plot of α_{eff} versus λ at a constant value of T_e shows that extrapolated values of α_{eff} at λ=0 gives nonzero negative values which are consistent with a non-zero loss factor $\beta(\lambda)$. In addition a minimum in α_{eff} at 10.49 μm is observed and is consistent with a maximum occuring in $\beta(\lambda)$ close to the oscillatory photoconductivity (OPC) condition $\hbar\omega=5\hbar\omega_L$. A strong ($\beta$=1) OPC effect is excluded because of the finite width of the excitation pulse $\sim\varepsilon_F+4k_BT_e$. The presently available range of photoexcitation energies from the CO_2 laser is not sufficient to expose other minima expected near $\hbar\omega=N\hbar\omega_L$ (N integer). Experiments are in progress on other concentration samples to investigate the physical origin of the non-zero loss factor β.

*Work supported in part by the Office of Naval Research.

Journal of Magnetism and Magnetic Materials 11 (1979) 247–252

SHUBNIKOV–DE HAAS EFFECT STUDIES ON OPTICALLY HEATED ELECTRONS IN n-InSb *

D.G. SEILER, L.K. HANES, M.W. GOODWIN and A.E. STEPHENS **
Department of Physics, North Texas State University, Denton, TX 76203, USA

Received 31 July 1978; in revised form 14 October 1978

CO laser-induced hot electrons in n-InSb at 1.8 K have been studied with the Shubnikov–de Haas effect which permits extraction of the electron temperature as a function of peak incident laser power.

1. Introduction

Hot electrons generated by dc electric fields in InSb have been widely studied using a number of experimental methods. However, optically induced hot electrons generated by intense laser radiation have been much less extensively investigated. Recently, the Shubnikov–de Haas (SdH) magnetoresistance oscillations have been used as a tool to determine the temperature of hot electrons produced by a CO_2 laser in degenerate n-InSm [1,2]. Only free carrier absorption processes needed to be considered because of the low intensity of the cw CO_2 laser and because the photon energy of the 10 μm CO_2 laser radiation is about half of the direct band gap energy E_g of InSb. In contrast, both intra- and inter-band effects are expected to be important in CO laser-induced hot electron effects in InSb where the photon energies can be tuned from below E_g to above E_g.

In this paper, we present the results of an investigation of the SdH effect in a sample of n-InSb irradiated with a CO laser. In section 2, we describe features of the SdH effect pertinent to its use in studying hot electrons. The experimental work, including sample properties and the apparatus, is given in section 3. The results and conclusions are then presented in section 4.

* Work supported in part by the Office of Naval Research.
** Permanent address: Department of Physics, Austin College, Sherman, TX 75090, USA.

2. The Shubnikov-de Haas effect

The Shubnikov–de Haas (SdH) effect is an oscillatory variation of magnetoresistance with magnetic field which can occur in a degenerate material at low temperatures. The conditions necessary for the SdH oscillations to be observed are $\omega_c\tau \gg 1$ and $k_B T_e < \hbar\omega_c < E_F$, where $\omega_c = eB/m^*c$ is the cyclotron frequency, τ is the lifetime of a state at the Fermi energy E_F, and T_e is the temperature of the electron gas, which may or may not be equal to the temperature of the lattice T_L. As the magnetic field B is increased, successive Landau levels rise past E_F and depopulate. As long as E_F remains constant, the magnetoresistance oscillations are periodic in B^{-1} with the period given by

$$P = \hbar e/E_F m^* c \,. \tag{1}$$

Provided the magnetic field does not become too large, the amplitude of the SdH oscillations in the longitudinal magnetoresistance of a material such as n-InSb can be expressed as [3,4]

$$A = \left(\frac{P}{2B}\right)^{1/2} \frac{\beta T_e m' \cos(\pi\nu)}{\sinh(\beta T_e m'/B)} \exp(-\beta T_D m'/B)\,, \tag{2}$$

where $\beta = 2\pi^2 k_B cm/\hbar e$, $m' = m^*/m$ is the ratio of effective mass to free electron mass, T_D is the Dingle or nonthermal broadening temperature, and ν is the spin splitting factor related to the effective g factor g^* by $\nu = m^* g^*/2m$.

Although the SdH oscillations can be observed with straightforward dc techniques, magnetic field

modulation and a lock-in amplifier are often used to improve the signal to noise ratio and to observe a larger number of oscillations When the lock-in amplifier is tuned to the modulation frequency, it measures an oscillatory signal with an envelope-to-envelope amplitude [5,6]

$$V = 4AJ_1(\alpha) \tag{3}$$

at a particular value of B. The argument of Bessel function J_1 is given by $\alpha = 2\pi B_M/PB^2$, where B_M is the amplitude of the modulation field.

The first hot electron SdH experiment in n-InSb was performed by Komatsubara [7], who applied large electric fields (>0.1 V/cm) to a 1.5×10^{15} cm^{-3} sample and observed a decrease in the SdH amplitude for the transverse configuration and a shift of the SdH extrema to higher B values as the electric field was increased. Later Isaacson and Bridges [8] studied a 1.7×10^{15} cm^{-3} sample of n-InSb and found that either an increase in the lattice temperature or an increase in the large electric field would decrease the transverse SdH amplitude and shift the extrema to higher B values. By matching the SdH curves for various lattice temperatures at a fixed low electric field with the curves for various high electric fields at a fixed low lattice temperature, Isaacson and Bridges determined the electron temperatures corresponding to given values of the electric field.

Bauer and Kahlert have investigated the hot electron SdH effect in n-InSb [9,10] (as well as in n-InAs [11] and n-GaSb [12]) using a pulsed electric field technique to avoid lattice heating [13]. For 5.9×10^{15} and 1×10^{16} cm^{-3} samples, T_D varied with T_L, so the T_e values for various electric fields were determined from the longitudinal oscillations by the direct comparison method used by Isaacson and Bridges [8]. For a 6.9×10^{16} cm^{-3} (more highly degenerate) sample, T_D was independent of T_L, so T_e values were obtained using

$$\frac{A(T_{e,1})}{A(T_{e,0})} = \frac{T_{e,1}\sinh(\beta T_{e,0}m'/B)}{T_{e,0}\sinh(\beta T_{e,1}m'/B)}, \tag{4}$$

from the amplitudes of longitudinal SdH oscillations. Little or no shift in the longitudinal SdH extremal positions was observed for these high concentration samples.

In the present study the conduction electrons were heated, not by a large electric field, but by optical excitation. For photon energies much less than the band gap energy E_g, carrier heating should take place due to free carrier absorption and thermalization by electron–electron collisions. For larger photon energies, carriers should also be excited from impurity levels and from the valence band into the conduction band. A radiation induced increase in the steady state concentration should raise E_F and decrease the SdH period. This would shift the SdH extrema to higher B values. Also, according to the work of Kalushkin et al. [14], even if the concentration remains constant, the B and T_e dependence of E_F caused by incomplete degeneracy should cause P to decrease and the extrema to move to higher B values as T_e is increased. To take period changes into account, we define the function

$$F \equiv \frac{V(T_{e,1}, P_1)\,P_0^{1/2}J_1(\alpha_0)}{V(T_{e,0}, P_0)\,P_1^{1/2}J_1(\alpha_1)}, \tag{5}$$

where V is given by eq. (3). If P, T_D, m', and ν are all constant, F is equal to eq. (4). The use of F in determining T_e values is given in section 4.

3. Experimental work

A block diagram of the experimental apparatus is shown in fig. 1. The laser is a sealed off, electric discharge cw CO laser capable of up to 2 W on many lines between 5.15 and 5.6 μm. The laser is grating tunable and has a short term ($\approx$1 s) amplitude stability of ±1% [15]. The TEM_{00} laser beam is passed through a Galilean type collimator to reduce the spot size and is then mechanically chopped to produce 20 μs wide pulses (F.W.H.M.) at a repetition rate of 1700 Hz. The 3.3% duty cycle of the chopper prevents lattice heating by the laser. The beam is focused onto the sample so that the region between the potential probes is as uniformly illuminated as possible. A He–Ne laser is used with a silicon PIN photodiode to produce a trigger pulse for the sampling oscilloscope. Calibrated filters are used after the chopper for beam attenuation.

The SdH oscillations are recorded using magnetic field modulation and sampling techniques developed by Kahlert and Seiler for pulsed experiments [16]. In the present work a constant dc current of 0.5 mA is applied to the sample. An ac magnetic field with

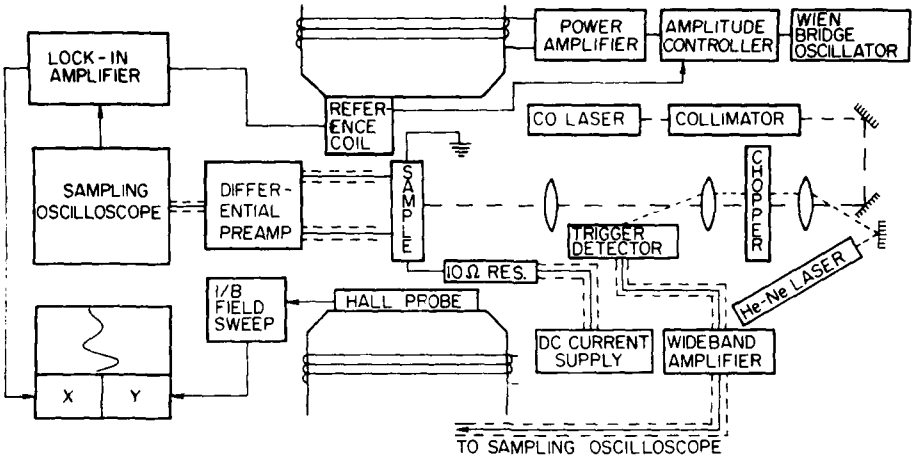

Fig. 1. Block diagram of experimental apparatus.

an amplitude of 75 G modulates the sample conductivity at a frequency of 43 Hz. The signal at the sample potential contacts, produced by the laser pulse and the field modulation, is fed through a high impedance differential amplifier into a Tektronix 7904/7S14 sampling oscilloscope. The output of the sampling oscilloscope is fed into a lock-in amplifier tuned to 43 Hz. The lock-in output is then plotted on an x-y recorder against $1/B$.

The sample was cut from a bulk specimen of n-InSb with an electron concentration of 1×10^{15} cm^{-3} and a Hall mobility of about 10^5 cm^2/Vs at 1.8 K. The front surface was optically polished with 0.3 μm Al_2O_3 polishing grit. The rear surface was left rough to eliminate multiple reflections and etalon effects. The sample dimensions were 5.63 mm × 1.65 mm × 0.1 mm thick. Two current contacts and two potential contacts were made using indium solder.

4. Results and conclusions

Fig. 2 shows SdH oscillations for lattice temperatures T_L of 1.8 to 11 K. It is quite apparent that the SdH amplitudes decrease with increasing values of T_L. One also observes a slight shift of the extrema to higher magnetic field positions as observed in previous SdH work by other authors [7,8,14]. This reflects an increase in electron temperature since the electrons are in equilibrium with the lattice during these measurements. The fact that ionized impurity scattering, which depends only on carrier energy, dominates the momentum relaxation in InSb below 40 K insures that the SdH amplitudes will be functions of electron temperature and not lattice temperature.

Fig. 3 shows several SdH traces taken with a constant T_L = 1.8 K. The bottom trace was taken with

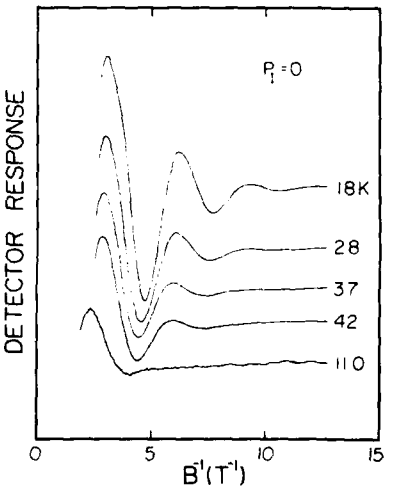

Fig. 2. SdH oscillations for various lattice temperatures without laser irradiation.

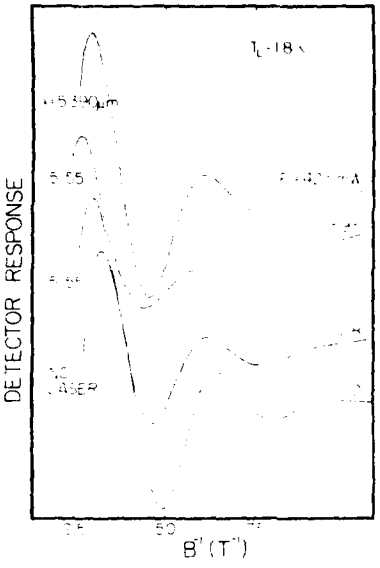

Fig. 3. Effect of laser irradiation at different wavelengths and incident powers on the SdH oscillations at constant lattice temperature.

the laser blocked (i.e., $P_I = 0$). For all wavelengths used, increasing the laser power decreases the SdH amplitudes and again a slight shift of the extrema to higher magnetic fields is generally observed. Lattice heating effects are not present during the time scales of the 20 μs laser pulses. This has been verified by measuring the electron temperature at different time positions during the 20 μs wide laser pulse. No changes in electron temperature were observed during the 20 μs where the laser power was constant. These measurements show that any lattice heating makes an insignificant contribution to the electron temperature for illumination on these time scales. The lattice time constants have been estimated elsewhere and are found to be on the order of milliseconds [17]. Thus the SdH oscillations are damped by increasing laser power in a similar manner to the damping caused by higher lattice temperatures. Also shown in fig. 3 is a SdH trace for $\lambda = 5.39$ μm for which $P_I = 42.5$ mW. The decrease in the SdH amplitude is less than that observed for $\lambda = 5.155$ μm with $P_I = 11.8$ mW even though the laser power is almost a factor of four greater. This indicates that the laser heating is certainly much greater for the shorter wavelength where

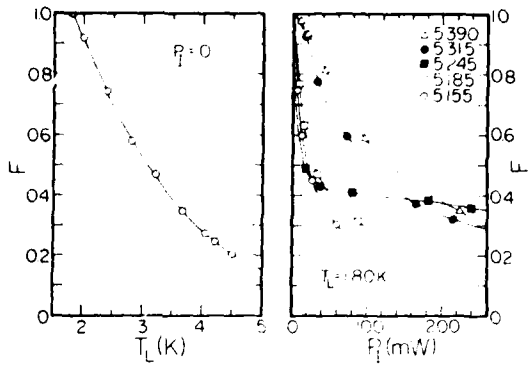

Fig. 4. Plots of the function F of eq. (5) vs. lattice temperature and peak incident laser power. The electron temperature is extracted by comparing the two graphs for a fixed value of F. The wavelengths are in micrometers.

the photon energy is greater than $E_g + E_F$. The direct gap is $\simeq$235 meV and the Fermi energy is $\simeq$2.5 meV.

Plots of the function F, defined in eq. (5), versus T_L and P_I can be used to determine the electron temperature for each particular wavelength and value of P_I as shown in fig. 4 by making a one-to-one correspondence between the two curves. An electron temperature can be extracted by the direct comparison method since the quantities compared are not explicit functions of the lattice temperature [18]. As noted earlier, this comparison method was first used by Issacson and Bridges [8] in high electric field measurements to extract electron temperatures from SdH

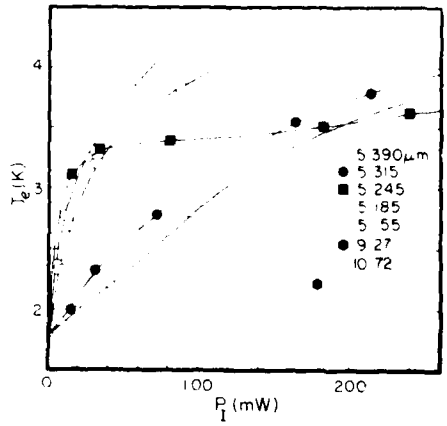

Fig. 5. Electron temperatures (from fig. 4) vs. peak incident CO laser power for different wavelengths at $T_L = 1.8$ K, together with CO_2 laser heating data.

data and has since been used extensively [19]. For example, for $\lambda = 5.315$ μm, a value of $P_I = 72$ mW corresponds to a temperature of about 2.8 K. The electron temperatures determined from the SdH data in this manner are shown in fig. 5, together with some results for the case of electron heating with a CO_2 laser. There is a quite striking non-linear behavior observed for all CO wavelengths. In addition, for $\lambda = 5.245$ μm an unusual dependence of T_e on P_I is seen, i.e., T_e rises rapidly and then remains relatively flat. At the highest powers used, a decrease of about 20% is observed in the SdH period at $\lambda = 5.245$ μm compared to the period at the other CO wavelengths.

Comparing the CO laser heating data with the CO_2 laser data shows that for fixed laser power T_e increases with decreasing wavelength in the 5 μm CO region while T_e increases with increasing wavelength for the two different wavelengths shown in the 10 μm CO_2 region. Clearly, different absorption processes are at work in the two spectral regions. Free carrier absorption mechanisms must be used to analyze the CO_2 laser data; this is obviously not the case with the current CO laser measurements.

Absorption in InSb in the 5 μm region is interesting, since it involves a variety of processes such as interband and impurity level transitions, and free carrier absorption. The results presented in fig. 5 are due to hot electron effects which involve these absorption processes. The results can be partially explained from a three level model consisting of a valence band, conduction band, and an acceptor level lying 7–10 meV above the valence band. The effects of free carrier absorption are negligible compared to those of direct interband and acceptor level absorption processes. The photoexcited electrons are created with an excess energy ΔE above the Fermi level by impurity level or interband transitions. The photoexcited electrons then heat the carriers in the conduction band via carrier–carrier scattering resulting in a quasi-equilibrium state with an increased electron temperature T_e.

The 5.39 and 5.315 μm wavelengths used correspond to photon energies of 230.2 and 233.5 meV respectively. These photon energies are sufficient to stimulate transitions from the acceptor level (but not the valence band) to the conduction band with a rather small ΔE remaining. T_e is seen to rise with P_I since the number of photoexcited electrons and hence the amount of electron heating is increased as P_I is increased. T_e finally appears to saturate due to depletion of the acceptor level; as there are only about 10^{13} cm^{-3} uncompensated acceptors, the change in concentration of a 10^{15} cm^{-3} n-type sample is limited to approximately 1%. T_e is higher for the higher photon energy line for a fixed P_I since here the excess energy ΔE is greater, so more heating occurs.

The photon energy of the 5.245 μm wavelength is 236.6 meV and is sufficient to excite acceptor level transitions but falls just short of being energetic enough to excite direct interband transitions at $T_e = 1.8$ K. However, the electrons excited from the impurity level have a larger excess energy than in the 5.315 μm case and therefore substantial heating of the electron gas occurs for small incident laser powers. As the electron gas in heated, the electron distribution function changes so that states are made accessible for direct interband transitions. Hence, initially at lower electron temperatures the direct transitions were forbidden, but after heating of the electron gas by the photoexcited electrons produced from the acceptor level, these transitions become possible. However, the electrons excited from the valence band have very little excess energy and thus make no significant contribution to the electron temperature. Thus, the electron temperature is seen to rise quickly and then level off as the acceptor levels are depleted and interband transitions commence.

This interpretation of the variation of the electron temperature with peak incident laser power is also confirmed by the observed changes in SdH period at 5.245 μm. The electron concentration (as determined by the SdH period) remains constant until the electron temperature reaches about 3.3 K at a peak laser power of ≈40 mW. Thereafter, the electron concentration increases with laser power. There is about a 25% increase in concentration when the laser power is increased from 40 mW to 240 mW, even though the electron temperature remains fairly constant over this range.

The two shortest wavelengths studied (5.185 and 5.155 μm) have photon energies of 239.3 and 240.7 meV which are sufficient to excite direct interband transitions with a significant ΔE remaining as well as acceptor level transitions. The absorption coefficient here becomes extremely large, so that the sample is no longer uniformly illuminated through its entire thickness. Instead, the radiation is absorbed almost

entirely in the first surface layers, resulting in intense carrier heating there. Consequently, T_e shows a rapid rise to high values for relatively small P_1.

The optical heating data presented here can be compared to that which is obtained using only pulsed, dc electric fields to heat the carriers. The increase of electron temperature with applied electrical power is controlled by energy loss rates of the conduction electrons to the lattice from some combination of deformation-potential, piezoelectric, or polar-optical phonon scattering. We find that it takes an applied electric field of $\simeq 70$ mV/cm to heat the conduction electrons up to an electron temperature of 5 K with the lattice at a temperature of 1.8 K. In contrast, the increase of electron temperature in the optical case is controlled by absorption and recombination processes, as well as the above energy loss rates.

In summary, Shubnikov–de Haas experiments have been used to determine the increase in temperature of the electron gas in InSb irradiated by a CO laser. The dependence of the electron temperature upon incident laser power and photon energy is shown to provide information on the absorption processes in InSb in the vicinity of the band gap. Further experiments using different concentration samples, higher powers, and more wavelengths will be performed to provide additional information on these absorption and hot carrier generation processes.

References

[1] B. Moore, D.G. Seiler and H. Kahlert, Bull. Am. Phys. Soc. 22 (1977) 460.
[2] B.T. Moore, D.G. Seiler and H. Kahlert, Solid-State Electron. 21 (1978) 247.
[3] A.E. Stephens, D.G. Seiler, J.R. Sybert and H.J. Mackey, Phys. Rev. B11 (1975) 4999.
[4] L.M. Roth and P.N. Argyres, in: Semiconductors and Semimetals, ed. R.K. Willardson and A.C. Beer (Academic Press, New York, 1966) Vol. I, Chap. 6, p. 159.
[5] A. Goldstein, S.J. Williamson and S. Foner, Rev. Sci. Instr. 36 (1965) 1356.
[6] D.G. Seiler, B.D. Bajaj and A.E. Stephens, Phys. Rev. B16 (1977) 2822.
[7] K.F. Komatsubara, Phys. Rev. Lett. 16 (1966) 1044.
[8] R.A. Isaacson and F. Bridges, Solid State Commun. 4 (1966) 635.
[9] G. Bauer and H. Kahlert, J. Phys. C6 (1973) 1253.
[10] H. Kahlert and G. Bauer, Phys. Rev. B7 (1973) 2670.
[11] G. Bauer and H. Kahlert, Phys. Rev. B5 (1972) 566.
[12] H. Kahlert and G. Bauer, Phys. Stat. Sol. 46(b) (1971) 535.
[13] A review of these and other electric field induced hot electron experiments is given by G. Bauer in: Springer Tracts in Modern Physics, ed. G. Höhler (Springer, New York, 1974) Vol. 74, p. 1.
[14] V.I. Kalushkin, E.A. Protasov, A.G. Rodionov and N.A. Toloknov, Fiz. Tekh. Poluprov. 8 (1974) 1786 [Sov. Phys. Semicond. 8 (1975) 1154].
[15] L.K. Hanes, M.S. Thesis, North Texas State Univ., Denton, TX (1977).
[16] H. Kahlert and D.G. Seiler, Rev. Sci. Instr. 48 (1977) 1017.
[17] C.D. Cantrell, J.F. Figueira, J.F. Scott and M.O. Scully, Appl. Phys. Lett. 28 (1976) 442.
[18] G. Bauer, in: Springer Tracts in Modern Physics, (Springer, Berlin, 1975) Vol. 74, p. 15.
[19] For example, see ref. [9–12].

Volume 28 number 3 OPTICS COMMUNICATIONS March 1979

ABSORPTION PROCESSES NEAR THE BANDGAP OF InSb: LASER-INDUCED HOT ELECTRON AND PHOTOCONDUCTIVITY STUDIES

D.G. SEILER and L.K. HANES
Department of Physics, North Texas State University, Denton, TX 76203, USA

Received 8 December 1978

CO laser-induced photoconductivity measurements in n-InSb at 1.8 K are shown to give information on the amount of carrier heating and the absorption processes near the bandgap. A model is presented to explain the observed dependence of the electron temperature on the incident photon energy and laser power. The model is shown to explain nonlinear absorption effects recently observed in InSb by Miller et al.

Optical absorption in InSb for photon energies near the bandgap energy is an interesting and as yet not fully understood phenomenon. In order to clarify the roles of the various absorption mechanisms we have measured the photoconductivity of n-InSb under irradiation from a mechanically chopped cw CO laser. The change in conduction electron mobility is calculated from the change in conductivity and an electron temperature is extracted by comparison with lattice temperature mobility measurements. A three level model used to describe Shubnikov-de Haas (SdH) hot electron measurements is shown to adequately describe the observed results [1].

Recently Miller et al. [2] reported the observation of non-linear optical effects using a cw CO laser as the light source. They found non linear index of refraction and absorption effects that became more pronounced for incident photon energies near the bandgap. In particular, at 4 K the absorption substantially decreased with increasing laser power for photon energies near the bandgap according to these authors. Linear absorption was only observed at intensities <1 mW/cm^2. Miller et al. ruled out heating of the crystal as a mechanism to explain these phenomena, but yet formulated no quantitative model to explain their data. We will show that our model not only explains our photoconductivity results but these nonlinear absorption effects as well.

The laser used is a sealed off, electric discharge cw CO laser capable of up to 2W on many lines having photon energies between 221.6 and 240.9 meV (5.6 to 5.15 μm). The laser is grating tunable and has a short term ($\sim$1 s) amplitude stability of $\pm 1\%$ [3]. The TEM_{00} laser beam is passed through a galilean type collimator to reduce the spot size and is then mechanically chopped to produce 20 μs wide pulses (fwhm) at a repetition rate of 1700 Hz. The 3.3% duty cycle of the chopper prevents lattice heating by the laser. The beam is focussed onto the sample so that the region between the potential probes is as uniformly illuminated as possible. A He-Ne laser is used with a silicon PIN photodiode to produce a trigger signal for the sampling oscilloscope. Calibrated filters are used after the chopper for beam attenuation.

The photoconductive voltage is measured using the sampling oscilloscope. The sample was cut from a bulk specimen of n-InSb with an electron concentration of 1×10^{15}cm^{-3}, a Hall mobility of about 10^5cm^2/Vs, and a dark conductivity of 19.3 (ohm-cm)$^{-1}$ at 1.8 K. The front surface was optically polished with 0.3 μm Al_2O_3 polishing grit. The rear surface was left rough to eliminate multiple reflections and etalon effects. The sample dimensions were 5.63 mm $\times$ 1.65 mm $\times$ 0.1 mm thick. Two current contacts and two poten-

tial contacts were made using indium solder.

The photoconductive voltage V_p was measured for five laser lines with photon energies from 230.2 to 240.7 meV. The measured photoconductive voltage is plotted for the various photon energies as a function of incident laser power in fig. 1. The 230.2 meV (5.390 μm) and 233.5 meV (5.315 μm) lines show a rise in V_p with P_I and appear to be leveling off. The other three lines show a somewhat different behaviour. We will show that different absorption and/or hot carrier generation processes are at work in these two cases.

The electron conductivity is $\sigma = ne\mu$ where n is the carrier concentration, e the electron charge, and μ the electron mobility. If σ_0, n_0, and μ_0 are the dark conductivity, concentration, and mobility respectively, then under photoexcitation we have $\sigma = \sigma_0 + \Delta\sigma = e(n_0 + \Delta n)(\mu_0 + \Delta\mu)$ so that the change in conductivity $\Delta\sigma$ to first order due to photoexcitation is $\Delta\sigma = e\mu\Delta n + en\Delta\mu$.

Since the direct gap of InSb is about 235 meV and the Fermi energy here is about 2.5 meV, the effective gap is about 237.5 meV. Thus for photon energies less than 237.5 meV direct interband transitions are forbidden and any change in n must come from impurity level transitions and is necessarily small, as the number of compensated acceptor states $N_A \ll N_D$, the number of donor states. Consequently for photon energies less than 237.5 meV we have $\Delta\sigma = ne\Delta\mu$.

For photon energies greater than about 237.5 meV, direct interband transitions as well as impurity level transitions are allowed and both μ and n can change substantially. Furthermore, since the absorption coefficient α increases several orders of magnitude over a narrow energy region for the interband transitions [4], the absorption is inhomogeneous even in the 100 μm thick sample studied here. This inhomogeneous absorption is the cause of the photo-conductive voltage for the 239.3 and 240.7 meV lines being lower than that of the sub bandgap energy 236.6 meV line. The incident laser radiation is absorbed entirely in the first surface layers, so that the rear side of the sample is essentially nonilluminated, resulting in a lower value of V_p than if the entire thickness was illuminated. A quantitative analysis of $\Delta\sigma$ for the highest photon energy lines will not be considered here.

The fractional change in conductivity $\Delta\sigma/\sigma$ is plotted in fig. 2b as a function of incident power for the 230.2, 233.5, and 236.6 meV photon energies. This

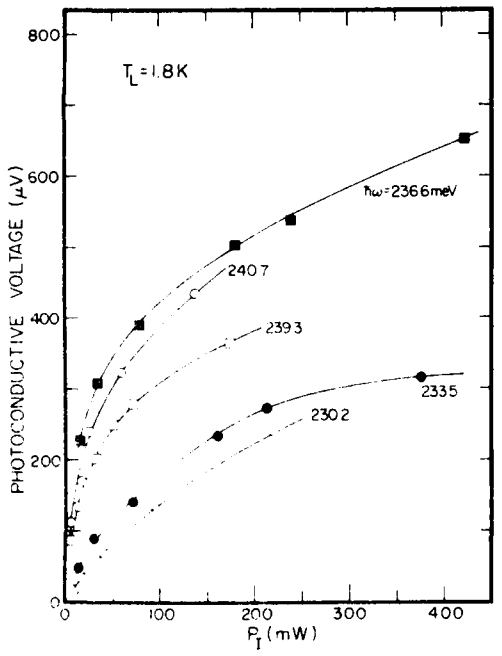

Fig. 1. Photoconductive voltage as a function of incident laser power for five CO laser photon energies.

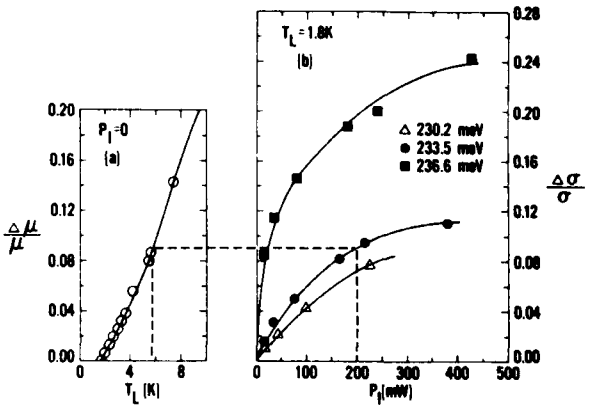

Fig. 2. (a) Fractional change in mobility as a function of lattice temperature at zero incident laser power. (b) Fractional change in conductivity due to photo excitation for three CO laser photon energies.

may be directly compared to the $\Delta\mu/\mu$ plot in fig. 2a for all points of the two lower energy lines, as n is known to remain essentially constant for all values of P_I from Shubnikov-de Haas measurements [1]. Thus an electron temperature can be extracted by a direct comparison of the two graphs since the quantities compared are not explicit functions of the lattice temperature [5]. This is due to the fact that ionized impurity scattering, which depends only on carrier energy, dominates the momentum relaxation in InSb below 40 K.

The 236.6 meV line is interesting, since it is known that for P_I above ≈50mW the electron concentration n does not change, while for P_I above ≈50mW n rises while T_e remains approximately constant [1]. Then for $P_I < \approx 50$ mW $\Delta\sigma/\sigma = \Delta\mu/\mu$. Thus the graphs can be used to extract an electron temperature for $P_I <$ ≈50 mW for this photon energy. Since $\mu \propto T_e$ and T_e remains constant for P_I greater than ≈50 mW, then in that region $\Delta\sigma/\sigma = \Delta n/n$. Since the hole mobility is very much less than the electron mobility, we can neglect the change in conductivity due to the change in hole concentration for the case of direct interband transitions. Calculations for $P_I > 50$ mW show about an 18% change in n, in agreement with the SdH data [1]. The absorption mechanisms for this photon energy are discussed more fully in the next section.

The electron temperatures extracted from fig. 2 are plotted for each photon energy as a function of P_I in fig. 3. The higher the photon energy, the greater the value of T_e for fixed P_I. The 230.2 and 233.5 meV line appear qualitatively similar, with the 233.5 meV line exhibiting a saturation at high values of P_I. It appears that the 230.2 meV line would saturate at higher incident power. The behaviour of the 236.6 meV line is completely different from the other two. The values of T_e extracted from the SdH measurements are lower than those shown in fig. 3 because the magnetic field is known to cool the electron gas [6].

A three level model consisting of the valence band, the conduction band, and an acceptor level lying 7–10 meV above the valence band is considered. For photon energies high enough to stimulate transitions from the valence band or impurity level to the conduction band the effects of free carrier absorption are negligible in comparison.

The photoexcited electrons are created with an excess energy of ΔE above the Fermi level by impurity level or interband transitions. The photoexcited electrons then heat the carriers in the conduction band via carrier-carrier scattering resulting in a quasi-equilibrium state with an increased electron temperature T_e. The model is illustrated in fig. 4.

At photon energies less than $E_G + E_F$ (bandgap energy plus Fermi energy) direct interband transitions are forbidden. However, if the photon energy is greater

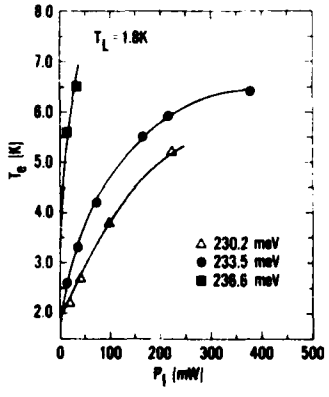

Fig. 3. Electron temperature as a function of incident laser power extracted by comparison of fig. 2a with fig. 2b.

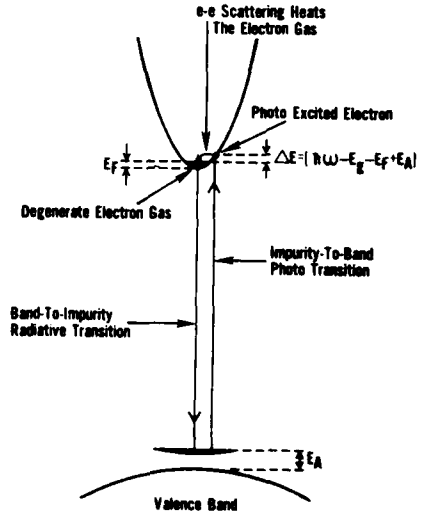

Fig. 4. Illustration of the three level model showing heating of the conduction electrons by photoexcited electrons from the impurity level.

than the energy gap between the impurity level and the top of the Fermi level ($\hbar\omega > E_G + E_F - E_A$, $E_A \sim 7 - 10$ meV [7]) then transitions between the impurity level and conduction band are possible. The photoexcited electrons heat the conduction electrons as described above. As the laser intensity is increased, more photoexcited electrons are produced until all the compensated acceptor states are depleted. At that point a saturation effect should be observed in the electron temperature, as no more electrons can be excited to the conduction band to produce heating of an electron gas.

For photon energies greater than $E_G + E_F$, both interband and impurity level transitions can occur. Owing to the large magnitude of the interband absorption coefficient, the interband transitions completely dominate over the impurity level transitions. In this case, absorption in the sample is no longer homogeneous and no saturation effect in T_e is expected or observed to occur.

At photon energies just slightly below the effective band gap (about 1 meV less than $E_G + E_F$) an interesting effect occurs. Initially interband transitions are forbidden, so that impurity level transitions alone heat the conduction electrons. As the laser power is increased, the heating of the electron gas causes the Fermi distribution to "tail off", resulting in states being made accessible for interband transitions. This induced absorption effect is illustrated in fig. 5. The electrons excited from the valence band have in effect a negative excess energy ΔE, since they arrive below the mean energy of the conduction electron gas. Hence the electron temperature should rise quickly with P_I and then level off as the induced interband absorption commences.

Using the three level model presented above, the decrease in absorption with increasing incident laser power observed by Miller et al. [2] is readily understood. They observed this effect at $\hbar\omega < E_G$ for a low concentration sample of n-InSb so that only impurity level transitions are allowed, and the absorption as well as the change in absorption became greater as the photon energy was increased.

As the incident laser power is increased, a rate equation analysis based on our model predicts that the number of compensated acceptor states available for absorption will become depleted, so that the absorptive transitions from the acceptor levels to the conduction band become inhibited. Thus the transmission should increase with increasing incident laser power. The effect becomes pronounced for higher photon energies since the absorption coefficient α_A is related to the photon energy $\hbar\omega$ and the concentration of ionized acceptors N_I by [8]

$$\alpha_A \propto N_I(\hbar\omega - E_G + E_A)^{1/2}/\hbar\omega ,$$

which increases with photon energy for energies approaching the bandgap. As the incident laser power is increased, then, N_I approaches zero and the absorption decreases.

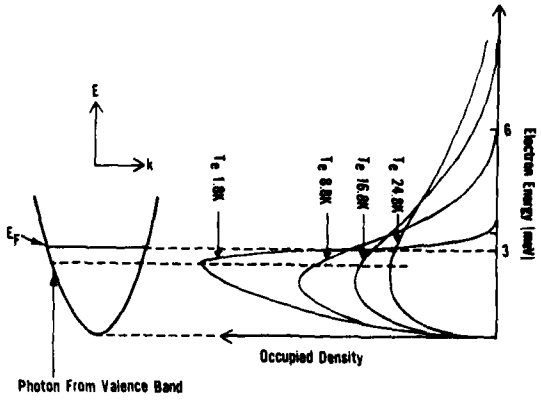

Fig. 5. Induced absorption by carrier heating for photon energies close to the effective bandgap energy.

On the basis of our model established from photoconductivity measurements and the form of the frequency dependence of the acceptor-transition absorption coefficient, it is clear that the absorption should decrease with increasing P_I and increase with photon energy, as observed by Miller et al.

In summary, photoconductivity measurements have been made for several photon energies both below and above the effective bandgap of InSb. By calculating the change in mobility of the conduction electrons due to photoexcitation, electron temperatures were extracted by comparison with measurements of the mobility as a function of lattice temperature. The hot electron measurements are shown to be able to directly provide information on the absorption processes in n-InSb for energies near the bandgap.

We acknowledge the financial support of this pro-

ject by the Office of Naval Research and would like to thank Dr. R.T. Bate for helpful comments.

References

[1] D.G. Seiler, L.K. Hanes, M.W. Goodwin and A.E. Stephens, J. Magn. and Magn. Mat., to be published.
[2] D.A.B. Miller, M.H. Mozolowski, A. Miller and S.D. Smith, Optics Comm. 27 (1978) 133.
[3] L.K. Hanes, M.S. Thesis, North Texas State University, December 1977, (unpublished).
[4] E.F. Johnson, Semiconductors and semimetals, Vol.3, (Academic Press, New York, 1967) p. 169.
[5] G. Bauer, Springer Tracts in Modern Physics, Vol. 74, (Springer, Berlin, 1975) p.15.
[6] G. Bauer, Springer Tracts in Modern Physics, Vol. 74, (Springer, Berlin, 1975) p.18.
[7] E.F. Johnson, Semiconductors and semimetals, Vol. 3, (Academic Press, New York, 1967) p.225.
[8] T.S. Moss, G.J. Burrell and B. Ellis, Semiconductor opto-electronics (Wiley, New York, 1973) p. 92.

NEW INTRABAND MAGNETO-OPTICAL STUDIES ON n-InSb

BY

D. G. SEILER AND M. W. GOODWIN

DEPARTMENT OF PHYSICS
NORTH TEXAS STATE UNIVERSITY
DENTON, TEXAS 76203

INVITED SEMINAR PRESENTED AT THE NATO ADVANCED STUDY INSTITUTE ON THEORETICAL ASPECTS AND NEW DEVELOPMENTS IN MAGNETO-OPTICS, ANTWERPEN, BELGIUM, JULY 16-27, 1979.

NEW INTRABAND MAGNETO-OPTICAL STUDIES ON n-InSb

D. G. Seiler and M. W. Goodwin

Department of Physics
North Texas State University
Denton, Texas 76203

Over the past 20 years magneto-optical studies in semiconductors have proven capable of accurately determining energy band parameters because of the optical transitions that occur between magnetically quantized electronic or impurity states. In addition, interesting features in the optical and photoconductive properties are observed that are caused by the electron-phonon interaction. Here we present some novel features of the magneto-optical properties of n-InSb that represent a new development to this well-established field of solid state physics. Resonances are observed in the CO_2 laser-induced magnetophotoconductivity whose positions depend strongly upon photon energy. The results provide the first direct evidence of emission of five optical phonons during the energy relaxation process of the photo-excited electrons created by a CO_2 laser in n-InSb. All observed transitions can be described with one single set of band parameters.

Because of the low carrier density the absorption coefficient is small ($\sim 10^{-2}$ cm^{-1}) and any direct measurement of the changes in transmission with magnetic field are extremely difficult to detect. However, photoconductivity measurements are capable of detecting weak magneto-optical transitions. A high photoconductive signal-to-noise ratio was obtained with the same experimental apparatus shown in the block diagram given in a recent paper by Seiler et al.[1] To our knowledge this is the first time magneto-optical data have been obtained while simultaneously using both sampling oscilloscope and lock-in amplifier techniques. The resonant structure is recorded using magnetic field modulation and sampling oscilloscope techniques developed by Kahlert and Seiler[2] for pulsed electrical experiments. However, it is also applicable to these magneto-optical studies and thus can be used to great advantage in improving signal-to-noise

ratios in photoconductivity measurements. In the present work a constant dc electrical current is applied to the sample while an ac magnetic field of amplitude 75 G modulates the sample conductivity at a frequency of 43 Hz. The photoconductive signal produced by the laser pulse and the field modulation is fed through a high impedence differential amplifier into a Tektronix 7904/7S14 sampling oscilloscope. The output of the sampling oscilloscope is fed into a lock-in amplifier tuned to 86 Hz which results in a lock-in detector response proportional to the second derivative of the photoconductive signal. The n-type InSb sample has a net carrier concentration at 1.8 K of about 2×10^{14} cm^{-3} as determined by Hall coefficient measurements. In all cases the electric field of the laser and the current through the sample are both parallel to the magnetic field direction.

Figure 1 shows reproductions of the output of the lock-in amplifier at 0 and 180 mW of peak incident laser power P_I for a wavelength of 9.24 μm and a lattice temperature T_L of 1.8 K. For all traces recorded a current of 5.5 mA is applied to the sample which puts the current-voltage characteristics well into the non-ohmic regime. This maximises the observed resonant structure. Traces taken with successively smaller currents down to 25 μA (well within the ohmic regime) show no changes in the positions of the optically induced structure. As the peak incident power is increased, a series of sharply defined resonant resistivity minima develop that are periodic in inverse magnetic field. This periodicity suggests some type of resonance behavior involving Landau Levels. Close inspection of

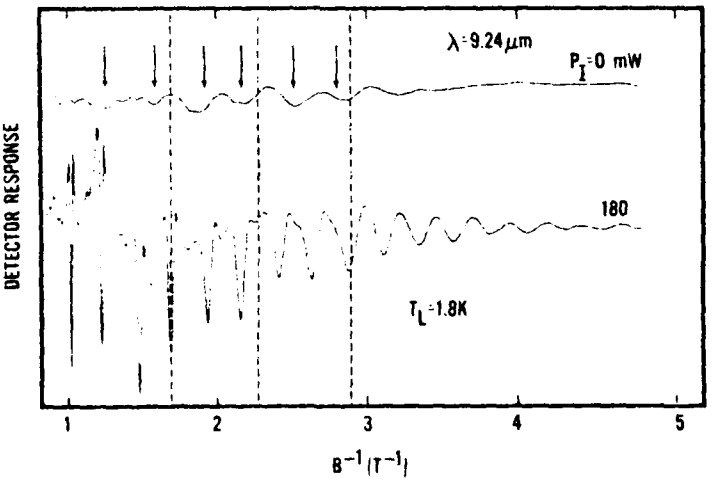

Fig. 1. Resonant magnetophotoconductivity spectrum at 180 mW of peak incident laser power. The arrows show the hot electron magnetophonon resonances observed as resistivity minima by Stradling and Wood[3] for $P_I = 0$.

the minima reveals an alternating series of oscillations which we identify as being caused by spin-splitting of the Landau levels. With increasing magnetic field, the resonant minima structure increases in amplitude and become much more sharply defined, a behavior typically associated with the density of states in a magnetic field.

The resonant minima structure exhibit a strong dependence on photon energy for wavelengths between 9.24 μm and 10.35 μm, as expected for Landau level related transition energies. For decreasing photon energies or increasing wavelengths as seen in Fig. 2, the periods of oscillation become larger, which shifts the minima positions to lower magnetic fields. The intraband transition energies at these resonance positions are plotted in the usual "fan chart" manner as shown in Fig. 3. These resonance positions extrapolate to a large energy value which we interpret as being 5 times the LO phonon energy, which means that the final E_F and initial E_i state energies of the electron differ by less than one LO phonon energy. Conservation of energy considerations lead to

$$\hbar\omega = E_F - E_i + m\hbar\omega_{LO} \quad , \tag{1}$$

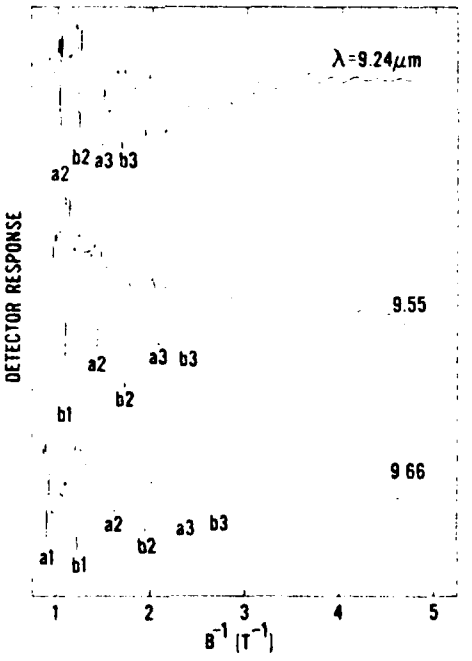

Fig. 2. Photoconductivity spectra for various CO_2 laser wavelengths. The structure is labeled by the final state Landau Levels as shown in Fig. 3, while a and b represent the spin up and spin down levels, respectively.

where $\hbar\omega$ is the photon energy, m is the integer equal to 5, and $\hbar\omega_{LO}$ is the LO phonon energy. Selection rules should not be important for these transitions as the optical transitions occur in very highly nonparabolic energy bands. We use Johnson and Dickey's model[4] to calculate the Landau energy level variation with magnetic field. We find that the calculated resonance positions do not agree very well with the observed positions if the lowest Landau level is chosen as the initial state and the final state is a higher Landau level.

At low electron concentrations and low temperatures InSb is well known to exhibit magnetic freeze out effects which occur when free electrons become more and more localized to the donor sites. Even moderate magnetic fields ($\leq$1T) produce binding energies ε_B of several meV. Consequently, we adopt a model where the initial state is a magnetically induced donor impurity level or impurity band just below the lowest Landau level. In all the Landau level calculations we have used the following band parameter values that were used or determined by Johnson and Dickey[4]: E_g = 236.7 meV, Δ = 810 meV, and a g-factor = -51.3. Even though ε_B has been shown to vary as $B^{1/3}$ for magnetic fields greater than 5 T,[5] we find that for the low magnetic fields used in this experiment, ε_B exhibits a behavior such that the impurity level or impurity band essentially remains stationary while the lowest Landau level moves up in energy by 1/2 $\hbar\omega_c$. The curved lines in Fig. 3 are calculated for m = 5, $\hbar\omega_{LO}$ = 23.6 meV and m^* = 0.0145 m_o. There is excellent agreement between the observed resonant positions and the theoretical lines. The value of the LO phonon energy is in reasonable agreement with the result of

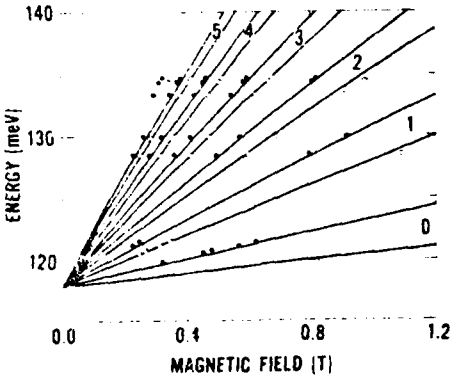

Fig. 3. Intraband transition energies versus magnetic field. The lines are calculated with parameters as discussed in the text. The numbers represent the Landau level number and the open circles and closed circles the spin up and spin down magnetic states, respectively.

24.4 ± 0.3 meV from Johnson and Dickey's work[4] and other determinations listed by Haas[6]. The band edge effective mass value of 0.0145 m_c also agrees quite well with other studies, as do the resulting values of g_B at these low magnetic fields.

The physical origin of the resonant spectroscopy effect in the magnetophotoconductivity is quite easy to understand and represents a novel application of the photoconductive "electron bolometer" effect or Putley hot electron detection principles to the study of intraband magneto-optics.[7] In this case, the photoconductivity is an excellent tool for the determination of transition energies and should be viewed as arising from the absorption processes in which the CO_2 laser radiation significantly changes the mobility rather than the number of free carriers. The initial state of the electron might be either the lowest Landau level or the donor impurity state with a magnetic field induced binding energy. An electron thus undergoes a transition taking it high into the Landau level conduction bands. Energy relaxation then takes place by the successive emission of longitudinal optical phonons leaving the electron in a final state of a Landau level. Which Landau level depends upon the magnetic field and the photon energy. The electron, in its final state, then interacts weakly with the lattice because of the dominance of ionized impurity scattering in n-InSb at low temperatures. It is thus possible to maintain a steady state for these electrons which have a mean energy appreciably greater than their thermal energy. Consequently, the conductivity increases. Fixing the photon energy and sweeping the magnetic field allows the observation of conductivity maxima in the photoconductivity signal which reflect the magnetic field quantization and singularities in the density of states.

The authors gratefully acknowledge the partial support of this research by the Office of Naval Research, the stimulating discussions with K. Ngai, and the helpful comments from B. D. McCombe and W. J. Moore.

1. D. G. Seiler, J. R. Barker, and B. T. Moore, Phys. Rev. Letters 41, 319 (1978).
2. W. Kahlert and D. G. Seiler, Rev. Sci. Instrum. 48, 1917 (1977).
3. R. A. Stradling and R. A. Wood, J. Phys. C., Sol. State 3, 2425 (1970).
4. E. J. Johnson and D. H. Dickey, Phys. Rev. B 1, 2676 (1970).
5. L. J. Neuringer, in Proceedings of 9th Int. Conf. on Phys. of Semiconductors, 1968 (Publishing House Nauka, Leningrad, 1968)
6. M. Haas, in Semiconductors and Semimetals, R. K. Willardson and A. C. Beer, eds. Vol. 3 (Academic Press, New York, 1967), p. 11.
7. See for example, E. H. Putley, in Semiconductors and Semimetals, R. K. Willardson and A. C. Beer, eds. Vol. 12 (Academic Press, New York, 1977), p. 143 and reference contained therein.

NEW INTRABAND MAGNETO-OPTICAL STUDIES ON n-InSb

D. G. Seiler, M. W. Goodwin
Department of Physics
North Texas State University
Denton, Texas 76203

and

K. Ngai
Naval Research Laboratories
Washington, D. C. 20375

ABSTRACT

A highly sensitive photoconductive technique has been used to provide the first direct evidence of emission of five optical phonons during the energy relaxation process of thephotoexcited electrons induced by a CO_2 laser in n-InSb. The CO_2 laser-induced magnetophotoconductivity exhibits a number of very sharp resonances whose positions depend strongly upon photon energy. All observed transitions can be described with one single set of band parameters.

Over the past 20 years magneto-optical studies in semiconductors have proven capable of accurately determining energy band parameters because of the optical transitions that occur between magnetically quantized electronic or impurity states. In addition, interesting features in the optical and photoconductive properties are observed that are caused by the electron-phonon interaction. These include such effects as oscillatory photoconductivity and phonon-assisted cyclotron resonance (PACR) harmonic transitions. In this letter we present some novel features of the magneto-optical properties of n-InSb that represent a new development to this old, well established field of solid state physics. A highly sensitive technique is used to record extremely sharp resonant structure in the magneto-photoconductivity induced by a CO_2 laser at much lower magnetic fields than have been used previously by other workers. The results directly show that the intraband magneto-optical transitions involve the subsequent emission of multiple longitudinal optical (LO) phonons.

The phenomenon is quite easy to understand and represents a novel application of the photoconductive "electron bolometer" effect or Putley hot electron detection principles to the study of intraband magneto-optics.[1] In this case, the photoconductivity is an excellent tool for the determination of transition energies and should be viewed as arising from the absorption processes in which the CO_2 laser radiation significantly changes the

mobility rather than the number of free carriers. The initial state of the electron might be either the lowest Landau level or the donor impurity state with a magnetic field induced binding energy. An electron thus undergoes a transition taking it high into the Landau level conduction bands. Energy relaxation then takes place by the successive emission of longitudinal optical phonons leaving the electron in a final state of a Landau level. Which Landau level depends upon the magnetic field and the photon energy. The electron, in its final state, then interacts weakly with the lattice because of the dominance of ionized impurity scattering in n-InSb at low temperatures. It is thus possible to maintain a steady state for these electrons which have a mean energy appreciably greater than their thermal energy. Consequently the conductivity increases. Fixing the photon energy and sweeping the magnetic field allows the observation of conductivity maxima in the photoconductivity signal which reflect the magnetic field quantization and singularities in the density of states.

Because of the low carrier density the absorption coefficient is small ($\sim 10^{-2}$ cm^{-1}) and any direct measurement of the changes in transmission with magnetic field are extremely difficult to detect. However, photoconductivity measurements are capable of detecting weak magneto-optical transitions. A high photoconductive signal-to-noise ratio was obtained with the same experimental apparatus shown in the block diagram given in a recent paper by Seiler et al.[2] To our knowledge this is the first time magneto-optical data have been obtained while simultaneously using both sampling

oscilloscope and lock-in amplifier techniques. The n-type InSb sample has a net carrier concentration at 1.8 K of about 2×10^{14} cm^{-3} as determined by Hall coefficient measurements. In all cases the electric field of the laser and the current through the sample are both parallel to the magnetic field direction.

The resonant structure is recorded using magnetic field modulation and sampling oscilloscope techniques developed by Kahlert and Seiler[3] for pulsed electrical experiments. However, it is also applicable to these magneto-optical studies and thus can be used to great advantage in improving signal-to-noise ratios in photoconductivity measurements. In the present work a constant dc electrical current is applied to the sample while an ac magnetic field of amplitude 75 G modulates the sample conductivity at a frequency of 43 Hz. The photoconductive signal produced by the laser pulse and the field modulation is fed through a high impedence differential amplifier into a Tektronix 7904/7S14 sampling oscilloscope. The output of the sampling oscilloscope is fed into a lock-in amplifier tuned to 86 Hz which results in a lock-in detector response proportional to the second derivative of the photoconductive signal.

Figure 1 shows reproductions of the output of the lock-in amplifier at various peak incident laser powers P_I for a wavelength of 9.24 μm and a lattice temperature T_L of 1.8 K. For all traces recorded a current of 5.5 mA is applied to the sample which puts the current-voltage characteristics well into the non-ohmic regime. This maximizes the observed resonant structure. Traces taken with

successively smaller currents down to 25 μA (well within the ohmic regime) show no changes in the positions of the optically induced structure observed. The structure present at $P_I = 0$ are hot electron magnetophonon resonances which have previously been observed by Stradling and Wood.[4] These authors found resistivity minima at the magnetic field positions shown by the arrows in Fig. 1. As clearly seen in Fig. 1, there is excellent agreement between our data and theirs. As the peak incident laser power is increased, a series of sharply defined resonant resistivity minima develop that are periodic in inverse magnetic field. This periodicity suggest some type of resonance behavior involving Landau Levels. Close inspection of the minima reveals an alternating series of oscillations which we identify as being caused by spin-splitting of the Landau levels. With increasing magnetic field, the resonant minima structure increases in amplitude and become much more sharply defined, a behavior typically associated with the density of states in a magnetic field.

The resonant minima structure exhibit a strong dependence on photon energy as seen in Fig. 2 for wavelengths between 9.22 μm and 10.35 μm, as expected for Landau level related transition energies. For decreasing photon energies or increasing wavelengths, the periods of oscillation become larger, which shifts the minimum positions to lower magnetic fields. The intraband transition energies at these resonance positions are plotted in the usual "fan chart" manner as shown in Fig. 3. These resonance positions extrapolate to a large energy value which we interpret as being 5 times the LO phonon energy. Conservation of energy considerations lead to

$$\hbar\omega = E_F - E_i + m\hbar\omega_{LO} , \qquad (1)$$

where $\hbar\omega$ is the photon energy, E_F and E_i are the final and initial state energies of the electron, m is the integer equal to 5, and $\hbar\omega_{LO}$ is the longitudinal optical phonon energy. Selection rules should not be important for these transitions as the optical transitions occur in very highly nonparabolic energy bands.

The data indicates that the final and initial states of the electron differ by less than one LO phonon energy. Consequently, we use Johnson and Dickey's model[5] to calculate the Landau energy level variation with magnetic field. We find that the calculated resonance positions do not agree very well with the observed positions if the lowest Landau level is chosen as the initial state and the final state is a higher Landau level.

At low electron concentrations and low temperatures InSb is well known to exhibit magnetic freeze out effects which occur when free electrons become more and more localized to the donor sites. Even moderate magnetic fields ($\leq$1T) produce binding energies ε_B of several meV. Consequently, we adopt a model where the initial state is a magnetically induced donor impurity level or impurity band just below the lowest Landau level. The resonance condition then becomes

$$\hbar\omega = E_F - (E_{ao} - \varepsilon_B) + m\hbar\omega_{LO} \qquad (2)$$

where E_{ao} is the lowest N = 0 spin split Landau level.

In all the Landau level calculations we have used the following band parameter values that were used or determined by Johnson and Dickey[5]: E_g = 236.7 meV, Δ = 810 meV, and a g-factor = -51.3. The theoretical relationship given in Eq. (2) can then be used to find values of m*, ϵ_B, and $m\hbar\omega_{LO}$ that give a best fit to the experimental data. Even though ϵ_B has been shown to vary as $B^{1/3}$ for magnetic fields greater than 5 T,[6] we find that for the low magnetic fields used in this experiment, ϵ_B exhibits a behavior such that the impurity level or impurity band essentially remains stationary while the lowest Landau level moves up in energy by 1/2 $\hbar\omega_c$. The curved lines in Fig. 3 are calculated for m = 5, $\hbar\omega_{LO}$ = 23.6 meV and m* = 0.0.145 m_o. There is excellent agreement between the observed resonant positions and the theoretical lines. The value of the LO phonon energy is in resonable agreement with the result of 24.4 ± 0.3 meV from Johnson and Dickey's work[5] and other determinations listed by Haas.[7] The band edge effective mass value of 0.0145 m_o also agrees quite well with other studies, as do the resulting values of ϵ_B at these low magnetic fields.

In summary we have presented sensitive photoconductive effects in n-InSb at the medium infrared wavelengths near 10 microns. Initially the high energy photo-excited electrons undergo a fast exchange of energy with the lattice through multiple LO phonon emissions. The electrons, now much reduced in energy, lie below the LO phonon emission energy threshold. The coupling of the electrons with the lattice then becomes so weak in this secondary stage that even for small electric fields (~1 V/cm) the steady

state energy of the carriers is appreciably greater than the thermal equilibrium value. A significant change of conductivity can therefore occur which results in photoconductivity in the manner as was discussed by Putley in the far infrared range of 100 μm. The physical picture in the second stage of the photoconductive phenomena at 10 μm, as observed in the present work, is a rather faithful image of the physical processes governing the InSb photoconductivity in the wavelength range of 100 to 1000 μm. We have employed this novel 10 μm photoconductivity technique to study the magnetic level structures and associated cyclotron-resonance transitions in the 100 μm energy range. The sharp and well-defined structure in the magnetophotoconductivity enables measurements of the Landau level structure at magnetic fields much lower than has been possible in previous far-infrared magneto-optical studies in the wavelength region around 100 μm.

The authors gratefully acknowledge the partial support of this research by the Office of Naval Research and the helpful comments from B. D. McCombe, W. J. Moore, and D. H. Kobe.

REFERENCES

1. See for example, E. H. Putley, in Semiconductors and Semimetals, R. K. Willardson and A. C. Beer, eds. Vol. 12 (Academic Press, New York, 1977), p. 143 and references contained therein.

2. D. G. Seiler, J. R. Barker, and B. T. Moore, Phys. Rev. Letters 41, 319 (1978).

3. H. Kahlert and D. G. Seiler, Rev. Sci. Instrum. 48, 1017 (1977).

4. R. A. Stradling and R. A. Wood, J. Phys. C., Sol. State 3, 2425 (1970).

5. E. J. Johnson and D. H. Dickey, Phys. Rev. B 1, 2676 (1970).

6. L. J. Neuringer, in Proceedings of 9th Int. Conf. on Phys. of Semiconductors, 1968 (publishing House Nauka, Leningrad, 1968), p. 715.

7. M. Haas, in Semiconductors and Semimetals, R. K. Willardson and A. C. Beer, eds. Vol. 3 (Academic Press, New York, 1967), p. 11.

FIGURE CAPTIONS

Figure 1. Photoconductive spectra for different peak incident laser power P_I. The arrows show the hot electron magnetophonon resonances observed as resistivity minima by Stradling and Wood.

Figure 2. Photoconductive spectra for different CO_2 laser wavelengths. In each case the peak incident laser power is somewhat different. The structure is labeled by the final state Landau levels shown in Fig. 3.

Figure 3. Intraband transition energies versus magnetic field. The lines are calculated from Eq. 2 with parameters as discussed in the text. The numbers represent the Landau level number, while a and b represent the spin up and spin down magnetic states, respectively.

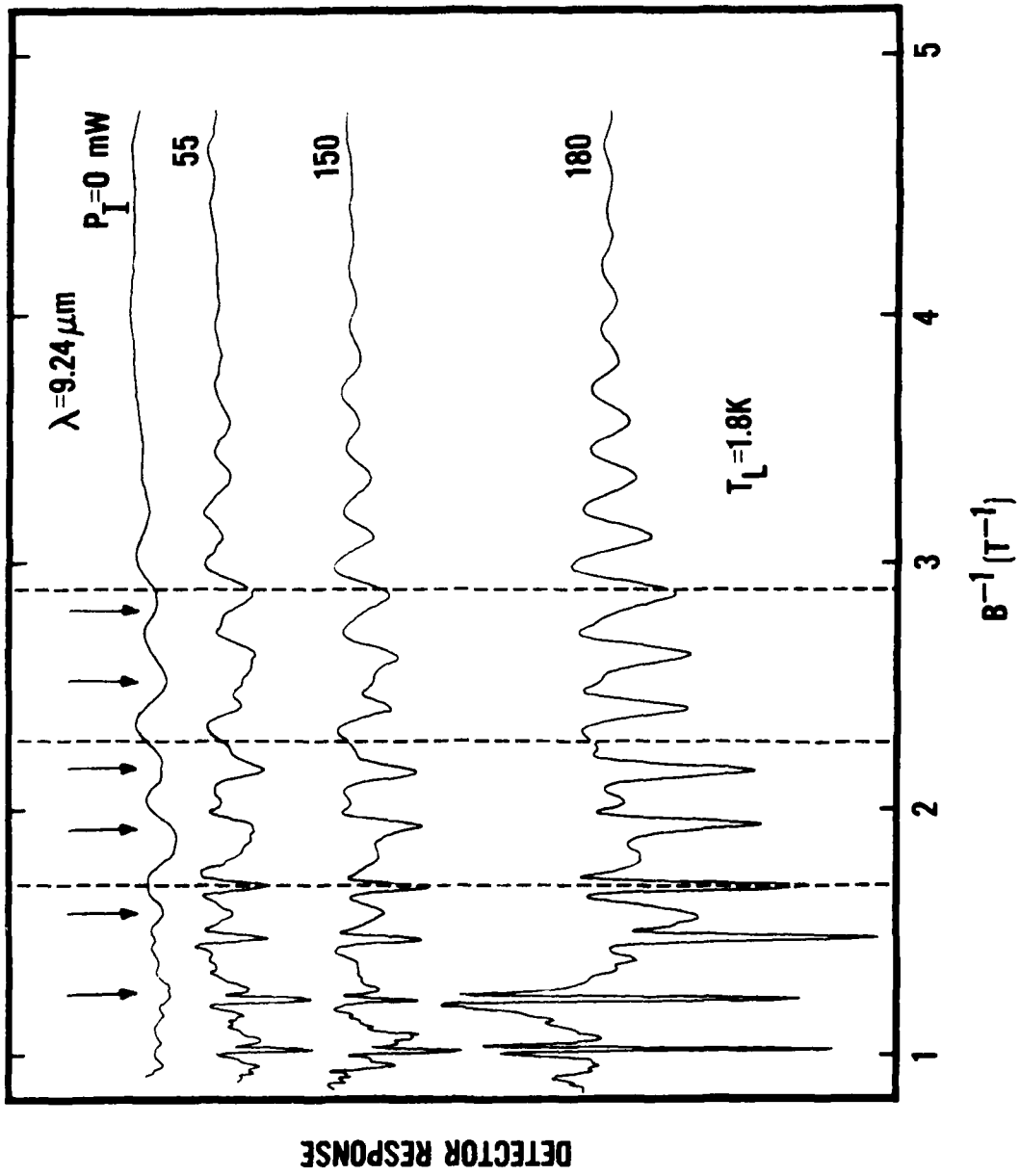
λ=9.24 μm
P_I=0 mW
55
150
180
T_L=1.8K
1
2
3
4
5
B^-1 (T^-1)
DETECTOR RESPONSE

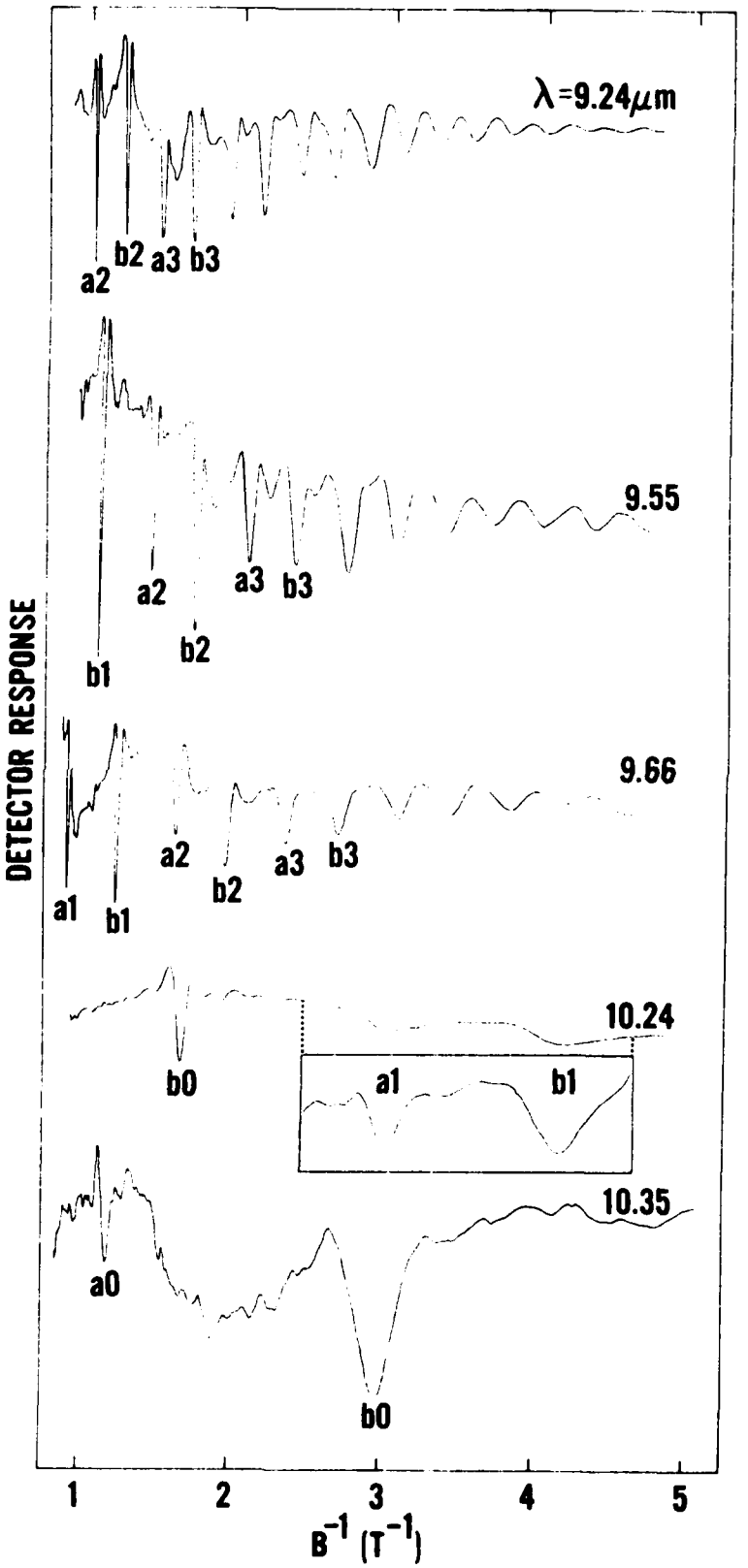
λ=9.24μm
a2
b2
a3
b3
9.55
b1
a2
a3
b3
b2
9.66
a1
b1
a2
b2
a3
b3
10.24
b0
a1
b1
10.35
a0
b0
DETECTOR RESPONSE
1
2
3
4
5
B^-1 (T^-1)

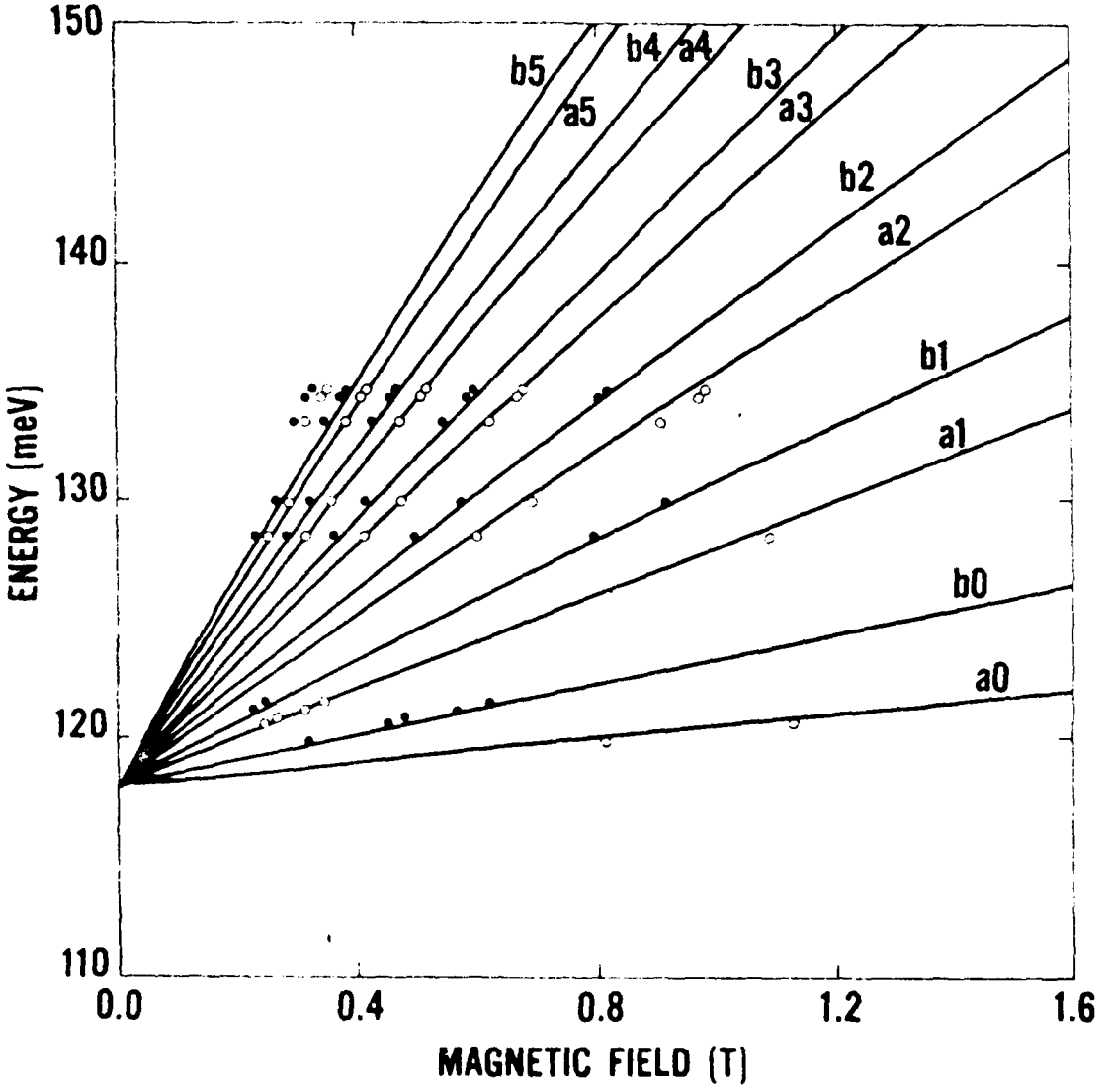
150
140
130
120
110
ENERGY (meV)
0.0
0.4
0.8
1.2
1.6
MAGNETIC FIELD (T)
b5
a5
b4
a4
b3
a3
b2
a2
b1
a1
b0
a0

THREE-PHONON ASSISTED CYCLOTRON HARMONIC TRANSITIONS IN THE MAGNETOPHOTOCONDUCTIVITY OF n-InSb

M. W. Goodwin, D. G. Seiler, and D. H. Kobe

Department of Physics, North Texas State University, Denton, Texas 76203

The CO_2 laser-induced magnetophotoconductivity of n-InSb (10^{14} cm^{-3}) at liquid helium temperatures exhibits resonant structure which depends upon the photon energy and the magnetic field. The resonant peaks are explained on the basis of a simple model in which an electron absorbs a photon and emits successively three LO phonons.

TO BE PUBLISHED IN SOLID STATE COMMUNICATIONS 36

Within the past decade magneto-optical experiments have proven capable of providing information on energy band structure in solids. The influence of the lattice on the magneto-optical properties is also quite significant and gives information on the electron-phonon interaction. In particular, phonon-assisted cyclotron resonance (PACR) experiments can yield valuable information concerning the electron-phonon coupling mechanism under the influence of a photon flux.[1] Because of the weak coupling, such experiments in n-type InSb have been primarily limited to one[1-4] and possibly two phonon[1,5,6] emission by the electron during photon absorption. In this paper we report resonant structure in the CO_2 laser-induced magnetophotoconductivity of n-InSb at liquid helium temperatures that can unambiguously be attributed to a three-phonon emission process.

The low concentration (9×10^{13} cm^{-3}) and the correspondingly low free carrier absorption coefficient (≈0.01 cm^{-1}) in the 10 μm spectral region prevents the observation of small changes in the transmission. However, photoconductivity measurements provide a much more sensitive means of determining small changes in the absorption. The measurements are done by using a variation on a combination of sampling oscilloscope and magnetic field modulation techniques.[7-9] The output of a grating-tuned cw CO_2 laser is mechanically chopped at 1500 Hz with a low duty cycle to prevent lattice heating. The resultant peak power is several hundred milliwatts.

A portion of the results of our studies for various wavelengths is shown in Fig. 1. The electric field of the laser and the current (I = 13 mA) through the sample are both parallel to the magnetic field direction. The detector response is proportional to the second derivative of the photo-induced magnetoresistance and is plotted against inverse magnetic field in units of inverse Telsa. The arrows point toward resistance minima and the numbers designate the final state Landau levels as shown in Fig. 2. The observed amplitudes of the resonant structure seen in Fig. 1 contain the effects of the magnetic field modulation method. Changes in the photoconductive voltage caused by resonances in the photo-induced magnetoresistance are clearly resolved in the data shown in Fig. 1. Notice that there is also a shift in the minimum positions to higher magnetic field with higher photon energies. This is consistent with Landau level related resonances as we will now show.

From an energy conservation point of view PACR is easily understood. As is usually stated, at resonance an electron occupying an initial state ε_i in the lowest N = 0 Landau level of the conduction band will absorb a photon of energy $\hbar\omega$ while successively emitting m longitudinal optical (LO) phonons of energy $\hbar\omega_o$ to arrive at some final higher Landau level ε_f. This resonance condition is usually stated as follows:

$$\hbar\omega = \varepsilon_f - \varepsilon_i + m\hbar\omega_o \quad . \tag{1}$$

Whenever the above equation is satisfied, resonant behavior in the photoconductivity occurs and may be observed if the right conditions exist.

To understand quantitatively the shift of the structure, the observed positions of the minima in the resistance (maxima in the conductivity) are plotted in Fig. 2 as a function of magnetic field for nine wavelengths between 10.27 and 10.81 μm. The lines represent our theoretical calculations based on Eq. (1) where we have used the Landau level model of Johnson and Dickey[4] along with their band parameters (g = -51.3, E_g = 236.7 meV, $m_c^* = 0.0139\ m_o$), to calculate ε_f and ε_i. The electron, initially in the lowest N = 0 spin up Landau level, is excited to the same spin state of some higher (N > 0) Landau level. The lines give the best fit to the data when m = 3 and $\hbar\omega_o$ = 24.5 meV. This value for the phonon energy is in excellent agreement with the value 24.4 meV determined by Johnson and Dickey.[4]

Also shown in Fig. 2 are the resonance positions observed in the photo-response of a sample of n-InSb irradiated by a CO_2 laser (117 meV) by Morita et al.[10] Even though their data was taken in a transverse configuration ($\vec{I} \perp \vec{B}$), it is in good agreement with our data and our theoretical calculations.

To understand qualitatively the origin of the resonant structure in the photoconductivity we must now discuss the nature of the electron distribution function and how it is related to the photoconductivity. The electron distribution function at low temperatures and in the presence of the laser radiation has been discussed by Levinson and Levinskii[11] for the case of zero magnetic field. They consider two energy regions: (1) an active region where $\varepsilon > \hbar\omega_o$ and emission of optical phonons predominates with a characteristic time $\tau_{PO} \approx 10^{-12}$ sec. and (2) a passive region where $\varepsilon < \hbar\omega_o$ and the emission of optical phonons is impossible. Energy relaxation in the passive region takes place through acoustic phonon scattering with a characteristic time $\tau_A \approx 10^{-8}$ sec. Electron-electron collisions dominate

in the passive region and thus a Maxwellian distribution can be established. However, the electron density is not sufficiently high for electron-electron collisions to dominate in the active region until a concentration of $10^{18}cm^{-3}$ is reached. Levinson and Levinskii[11] have described the energy distribution of the photo-excited electrons and given a form of the electron distribution function which exhibits peaks in the active region due to the cascade emission of optical phonons.

The observed photo-induced resonant structure involves three phonons and therefore must be produced by a fourth-order process involving the electron-radiation H_R and the electron-lattice H_L interactions. In deriving the transition rate due to the intraband magnetoabsorption it is helpful to consider the Feynman diagram in Fig. 3. The transition rate can be obtained in the usual manner by Fermi's Golden Rule which gives the probability per unit time that a transition is induced by a photon from the initial electron state $|k_i, \varepsilon_i\rangle$ to a final electron state $|k_f, \varepsilon_f\rangle$ with the emission of three LO phonons,

$$W_{i\to f} = \frac{2\pi}{\hbar} \sum_f |M_{fi}|^2 \, \delta(\varepsilon_f - \varepsilon_i - \hbar\omega + 3\hbar\omega_o) \quad , \qquad (2)$$

where a sum over the appropriate final states is indicated. We assume that only LO phonons at the zone center are involved and their dispersion can be neglected. The transition matrix element corresponding to Fig. 3 is

$$M_{fi} = \sum_{\alpha,\beta,\gamma} \frac{\langle f|H_L|\gamma\rangle\langle\gamma|H_L|\beta\rangle\langle\beta|H_L|\alpha\rangle\langle\alpha|H_R|i\rangle}{(E_i - \varepsilon_\gamma - 2\hbar\omega_o)(E_i - \varepsilon_\beta - \hbar\omega_o)(E_i - \varepsilon_\alpha)} \quad , \qquad (3)$$

where the sum is over all intermediate states α, β, γ, and $E_i = \varepsilon_i + \hbar\omega$. The energy of the electron in state α is ε_α, etc. There are three other diagrams, similar to Fig. 3, in which one or more phonons are emitted before the photon is absorved. At low temperatures phonon absorption processes can be neglected.

If the summation is replaced by an integral over the energy, Eq. (2) becomes

$$W_{i\to f} = \frac{2\pi}{\hbar} |M_{fi}|^2 \, g(\varepsilon_f) g_{3\text{phonons}} \quad , \qquad (4)$$

where $g(\varepsilon_f)$ is the density of the electrons at the final electron energy $\varepsilon_f = \varepsilon_i + \hbar\omega - 3\hbar\omega_o$, and $g_{3\text{phonon}}$ is the constant density of states for the three phonons.

The absorption coefficient can then be written as

$$K(\omega) = n \left\langle \frac{W_{i\to f}}{\text{Flux of photons}} \right\rangle_i , \qquad (5)$$

where the flux of photons = $N(\omega)\ c/\sqrt{\varepsilon(\omega)}$ and $\langle\ \rangle_i$ denotes the average over initial states. Here n is the electron concentration, $N(\omega)$ is the number of photons per unit volume with frequency ω, and $c/\sqrt{\varepsilon(\omega)}$ is the velocity of light in the medium, where $\varepsilon(\omega)$ is the real part of the dielectric constant. The averaging over initial states produces a convolution of the density of states with the result that

$$K(\omega) = \frac{n\sqrt{\varepsilon(\omega)}}{N(\omega)\ N_T} \int_0^\infty d\varepsilon_i g(\varepsilon_i) f(\varepsilon_i)$$

$$\times \frac{2\pi}{\hbar} |M_{fi}|^2\ g(\varepsilon_f) g_{3\text{phonons}} , \qquad (6)$$

where

$$N_T = \int_0^\infty d\varepsilon_i\ g(\varepsilon_i) f(\varepsilon_i)$$

is the total number of electrons present. Consequently, the absorption coefficient contains singularities due to the presence of singularities in the density of initial and final states. If some of the energy denominators in Eq. (3) for M_{fi} are small, the transition matrix element can also exhibit resonances. However, the data seems to indicate that such matrix element resonances are not significant. Thus, if either the photon energy is fixed and the magnetic field is varied or if the magnetic field is held constant and the photon energy varied, resonant structure in K should be observed. The photoexcited generation rate is directly proportional to the product of the absorption coefficient given in Eq. (6) and the optical intensity. Thus, the generation rate contains the density of states singularities. Initially, this generation rate into the final electron state is much greater than the energy loss rate out of the final electron state. However, in steady state the two rates become equal and a steady state distribution function results. Consequently, the distribution function in the presence of laser light exhibits peaks at certain energies just as in the case presented by Levinson and Levinskii.

If we define an effective relaxation time which is only a function of the electron energy, the photoconductivity $\Delta\sigma_{zz}$ in the longitudinal case for sufficiently low electric field is approximately

$$\Delta\sigma_{zz} = \frac{-e^2}{\Omega} \sum_{N,k_z} \frac{\partial(f - f_o)}{\partial\varepsilon}\ \tau_{eff}(\varepsilon)\ v_z^2(\varepsilon) , \qquad (7)$$

where e is the electronic charge, Ω is the volume of the crystal, f is the distribution function in the presence of the laser, f_o is the distribution function in the absence of the laser, ε is the electron energy, $v_z(\varepsilon)$ is the z-component of the electron velocity which is dependent upon energy, τ_{eff} is the relaxation time dominated by ionized impurity scattering (which varies as $\varepsilon^{3/2}$) and the sum is over all electron states.

Using a very simple model, we can approximate the difference in the distribution function with a sharp peak at the final electron energy ε_f of width approximately equal to the spread in the initial electron energies. If we approximate this peak by a δ function, we have

$$f - f_o \simeq N_f \, \delta(\varepsilon - \varepsilon_f) \quad . \tag{8}$$

The number of electrons in the final state N_f is related to the steady state condition where the generation rate equals the loss rate out of this state and must be $<< N_T$, the total number of electrons. If broadening were included, the delta function could be replaced in the usual manner with a Lorentzian shape distribution. Inserting Eq. (8) for $f - f_o$ into Eq. (7) and doing the integration over the derivative of the delta function, we get

$$\Delta\sigma_{zz} \propto \frac{d}{d\varepsilon} \left[g(\varepsilon) \, N_f \, \tau_{eff} \, v_z^2 \right]\Big|_{\varepsilon=\varepsilon_f} \quad . \tag{9}$$

This expression thus gives a contribution to the photoconductivity only at the resonant condition $\varepsilon = \varepsilon_f = \overline{\varepsilon}_i + \hbar\omega - 3\hbar\omega_o$, where $\overline{\varepsilon}_i$ is the average initial electron energy. This resonance condition $\varepsilon = \varepsilon_f = \overline{\varepsilon}_i + \hbar\omega - 3\hbar\omega_o$ is the same as Eq. (1) with $m = 3$, and an average initial electron energy in the N = 0 Landau level. The observed background photoconductivity is due in part to the depletion of the tail of the Maxwellian distribution by the photoexcitation of electrons. This effect has been neglected in Eq. (8) for simplicity, since the positions of the resonances is of primary concern here.

In summary, three-phonon assisted cyclotron harmonic transitions observed in the magnetophotoconductivity of n-InSb have been investigated. At present further investigations into multiple phonon assisted cyclotron harmonic transitions are in progress.

Acknowledgements -- We acknowledge the partial support of this research by the Office of Naval Research and a Faculty Research Grant from NTSU. We wish to thank E. J. Johnson, B. D. McCombe, A. Miller, and A. L. Smirl for their helpful comments.

REFERENCES

1. V. I. Ivanov-Omskii, L. I. Korovin, and E. M. Shereghii, Physica Status Solida (b) 90, 11 (1978).
2. R. Grisar, Physical Review B 18, 4355 (1978).
3. R. C. Enck, A. S. Saleh, and H. Y. Fan, Physical Review 182, 790 (1969).
4. E. J. Johnson and D. H. Dickey, Physical Review B 1, 2676 (1970).
5. K. L. Ngai and E. J. Johnson, Physical Review Letters 29, 1607 (1972).
6. J. T. Devresse, Physical Review B 17, 3207 (1978).
7. H. Kahlert and D. G. Seiler, Review Scientific Instruments 48, 1017 (1977).
8. B. T. Moore, D. G. Seiler, and H. Kahlert, Solid State Electronics 21, 247 (1978).
9. D. G. Seiler, L. K. Hanes, M. W. Goodwin, and A. E. Stephens, Journal of Magnetism and Magnetic Materials 11, 247 (1979).
10. S. Morita, S. Takano, and H. Kawamura, Solid State Communications 12, 247 (1973).
11. Y. B. Levinson and B. N. Levinskii, Soviet Physics JETP 44, 156 (1976).

FIGURE CAPTIONS

Fig. 1 - Detector response as a function of inverse magnetic field for four CO_2 laser wavelengths. The lattice temperature is 1.8 K. N is the final state Landau level number.

Fig. 2 - Intraband transition energies versus magnetic field. Theoretical transitions calculated from Eq. (1) are shown as lines. Experimental values: •our work showing resistance minima; *photoresponse data (Ref. 10).

Fig. 3 - The Feynman diagram corresponding to the absorption of a photon and the emission of three LO phonons. The initial state of the electron is k_i with energy ε_i, and the final state is k_f with energy ε_f. The photon, represented by the wavy line, has wave vector $\vec{k}$ and angular frequency ω. The LO phonons, represented by the dashed lines, have wave vectors $\vec{q}_1$, $\vec{q}_2$, and $\vec{q}_3$, with constant angular frequency ω_o. There are three other similar diagrams describing the processes in which one or more phonons are emitted before the photon is absorbed.

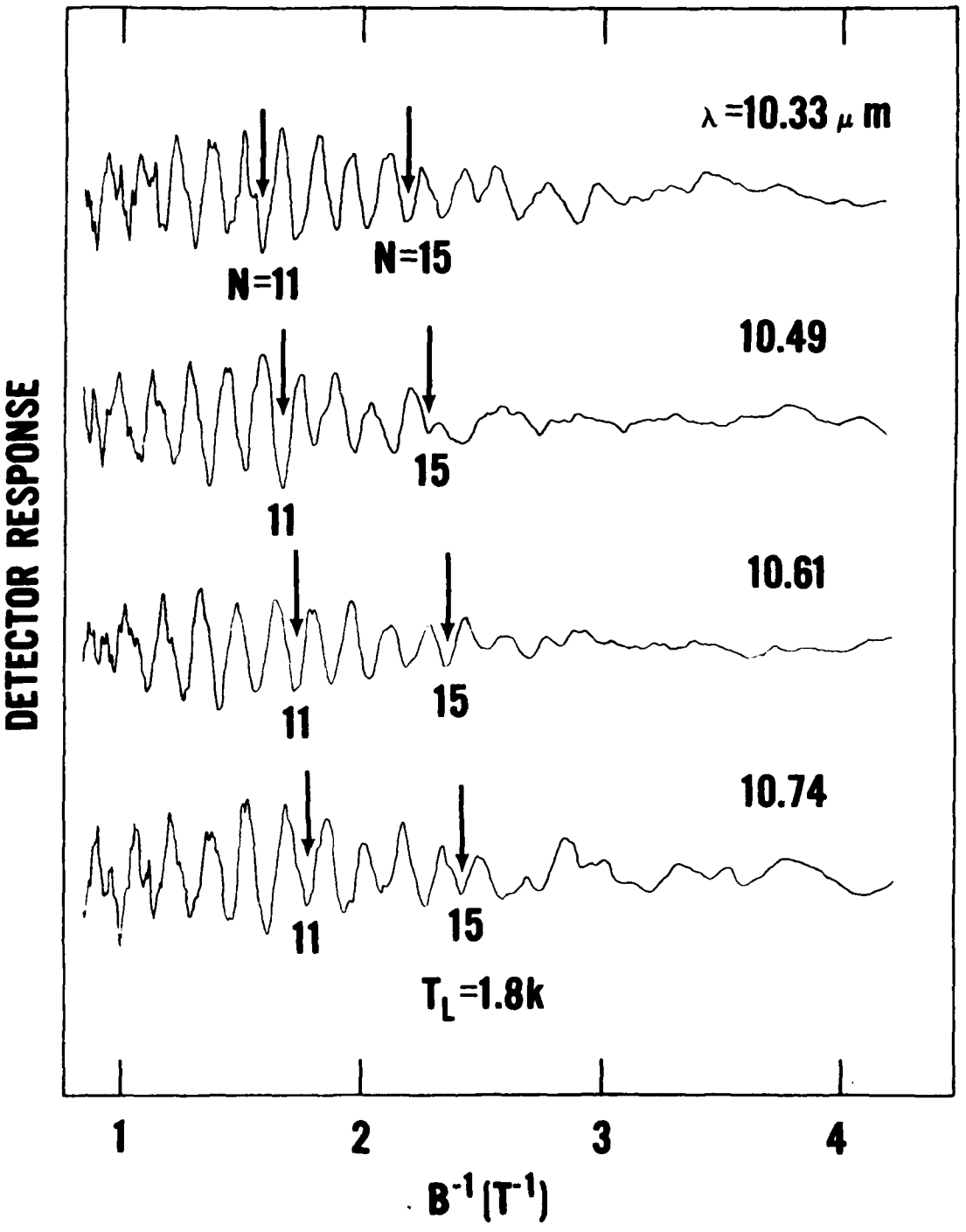
λ =10.33 μ m
N=11
N=15
10.49
11
15
10.61
11
15
10.74
11
15
T_L =1.8k
DETECTOR RESPONSE
1
2
3
4
B^-1 (T^-1)

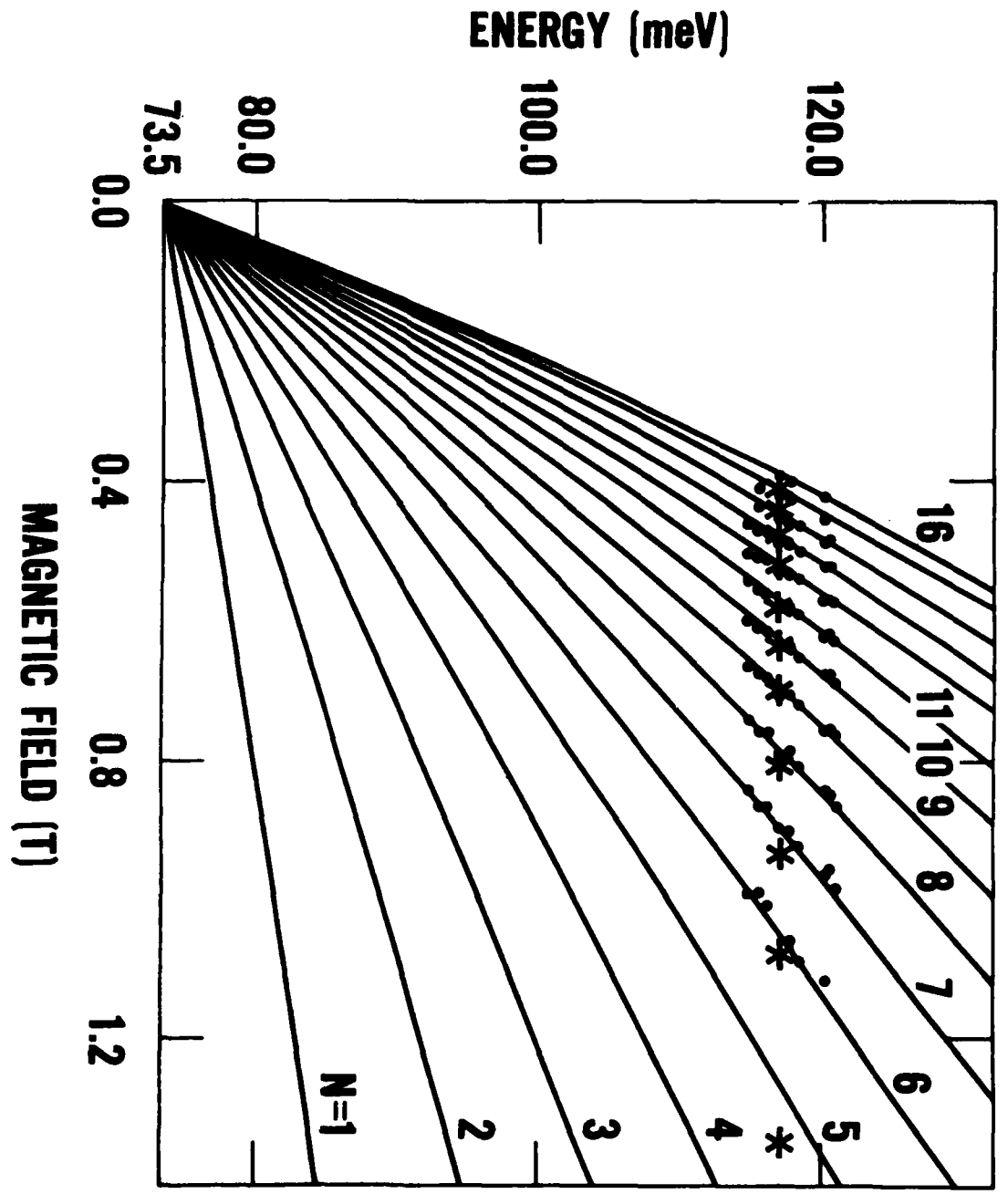
ENERGY (meV)
73.5
80.0
100.0
120.0
0.0
0.4
0.8
1.2
MAGNETIC FIELD (T)
N=1
2
3
4
5
6
7
8
9
10
11
16

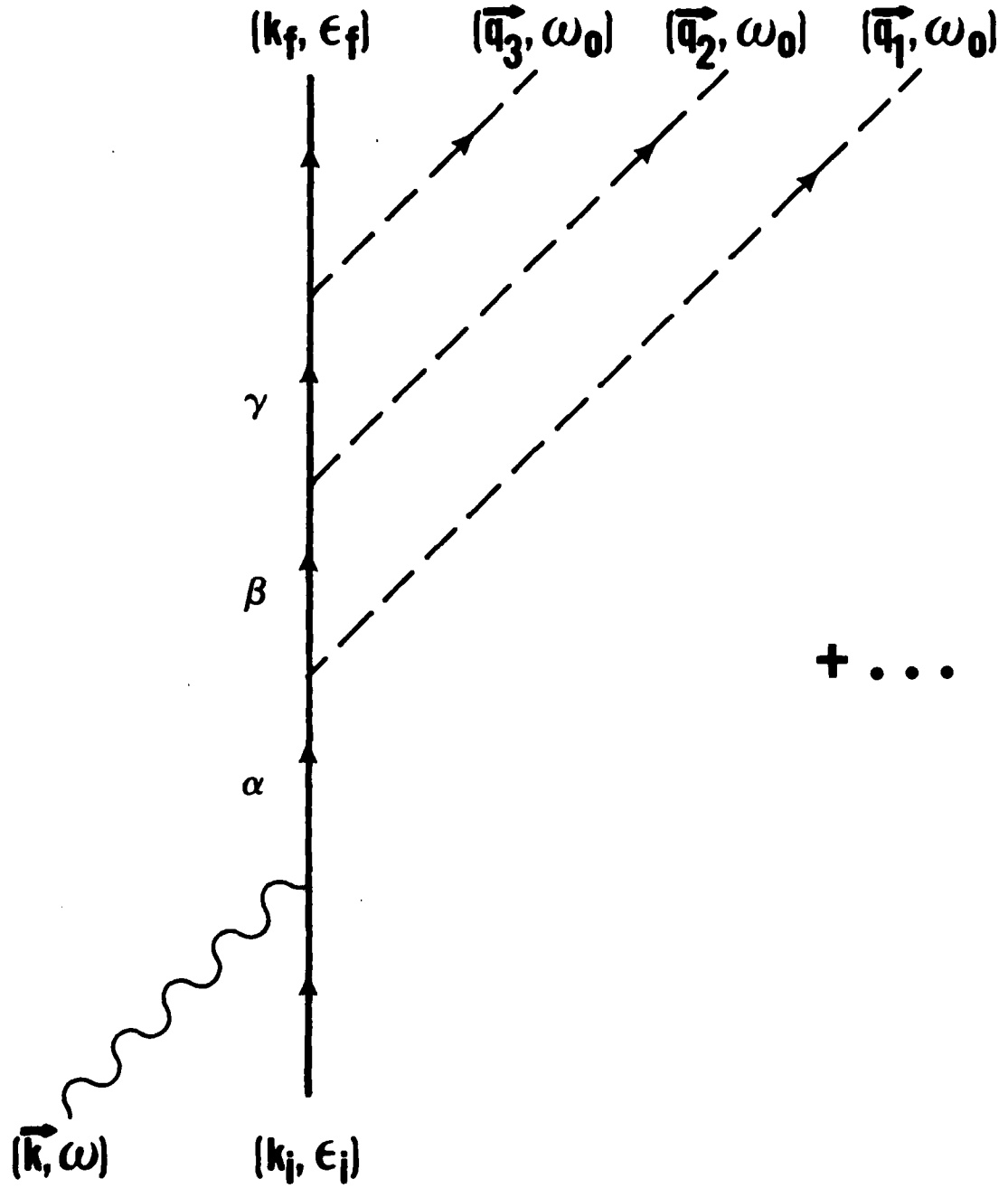
(k_f, ϵ_f)
$(\vec{q}_3, \omega_0)$
$(\vec{q}_2, \omega_0)$
$(\vec{q}_1, \omega_0)$
γ
β
α
+ . . .
$(\vec{k}, \omega)$
(k_i, ϵ_i)

Abstract Submitted

for the New York Meeting of the

American Physical Society

March 24-28, 1980
Date

Physics and Astronomy
Classification Scheme
Number 78, 72.40

Suggested title of session in which paper should be placed
1. Optical Properties of Semiconductors
2. Photovoltaic and Photoconductive Effects

New CO_2 Laser-Induced Magneto-optical Transitions in n-InSb.* M. W. GOODWIN and D. G. SEILER, North Texas State University--A highly sensitive photoconductivity measurement technique has allowed the observation of weak resonant structure in the magnetophotoconductivity at low magnetic fields. Two distinct sets of resonant structure are present, both of which are periodic in inverse magnetic field and have amplitudes which depend upon laser power, laser frequency, and the lattice temperature. At low laser powers spin-conserving transitions dominate and can be explained by a model in which an electron absorbs a photon and emits successively three LO phonons. At high laser powers larger amplitude resonant structure dominates and is characterized by transitions to both spin states of the final Landau level. Possible origins of this structure are presented and discussed.

*Supported by the Office of Naval Research and a Faculty Research Grant from N.T.S.U.

( ) Prefer Poster Session
(X) Prefer Standard Session
( ) No Preference

Signature of APS Member

M. W. Goodwin
Physics Department
North Texas State University
Denton, Texas 76203

Abstract Submitted

for the New York Meeting of the

American Physical Society

March 24-28, 1980
Date

Physics and Astronomy
Classification Scheme
Number 72.40, 78

Suggested title of session
in which paper should be placed
1. Photovoltaic and Photoconductive Effects
2. Optical Properties of Semiconductors

CO Laser-Induced Cooling of the Conduction Electrons in n-InSb.* L. K. HANES and D. G. SEILER, North Texas State University.--We report the first observation to our knowledge of a laser-induced cooling effect in a semiconductor. This cooling effect results from a combination of an applied dc electric field together with illumination by a CO laser. The conduction electrons are heated by a high electric field, altering the electron distribution so that injection of photoexcited electrons at energies below the unilluminated mean energy is possible by a photon of appropriate energy. The resulting decrease in mean energy manifests itself in both photoconductivity and Shubnikov-de Haas effect measurements in a sample of degenerate ($n = 1.3 \times 10^{15}$ cm^{-3}) n-InSb at 1.8 K. The dependence of this cooling effect on incident photon energies (229.4 - 233.9 meV) and the role of acceptor impurity levels are discussed and a model is presented to explain the results.

*Supported by the Office of Naval Research and a Faculty Research Grant from N.T.S.U.

( ) Prefer Poster Session
(X) Prefer Standard Session
( ) No Preference

Larry K. Hanes
Signature of APS Member

Larry K. Hanes
Physics Department
North Texas State University
Denton, Texas 76203